Conformations of the Human Immunodeficiency Virus (HIV-1) Envelope Glycoproteins in Detergents and Styrene-Maleic Acid Lipid Particles (SMALPs)

Rong Zhou[1,2,6#], Shijian Zhang[1,2#*], Hanh T. Nguyen[1,2], Haitao Ding[3,4], Althea Gaffney[5], John C. Kappes[3,4], Amos B. Smith III[5], Joseph G. Sodroski[1,2*]

[1]Department of Cancer Immunology and Virology, Dana-Farber Cancer Institute, Boston, MA 02215, USA

[2]Department of Microbiology, Harvard Medical School, Boston, MA 02115, USA

[3]Department of Medicine, University of Alabama at Birmingham, AL 35294, USA

[4]Birmingham Veterans Affairs Medical Center, Research Service, Birmingham, AL 35294, USA

[5]Department of Chemistry, University of Pennsylvania, Philadelphia, PA 19104, USA

[6]Current affiliation: Department of Cardiology, The Second Affiliated Hospital of Shanxi Medical University, Taiyuan, Shanxi, China

[#]These authors contributed equally

*Corresponding authors:
Shijian Zhang, Ph.D.
Joseph G. Sodroski, M.D.
Dana-Farber Cancer Institute
450 Brookline Avenue, CLS 1010
Boston, MA 02215
Phone: 617-632-3371 Fax: 617-632-4338
Email: shijian_zhang@dfci.harvard.edu, joseph_sodroski@dfci.harvard.edu

Running title: HIV Env conformations in detergents or SMALP nanodiscs

Abstract word count: 249

Importance word count: 149

ABSTRACT

The mature human immunodeficiency virus (HIV-1) envelope glycoprotein (Env) trimer, which consists of non-covalently associated gp120 exterior and gp41 transmembrane subunits, mediates virus entry into cells. The pretriggered (State-1) Env conformation is the major target for broadly neutralizing antibodies (bNAbs), whereas receptor-induced downstream Env conformations elicit immunodominant, poorly neutralizing antibody (pNAb) responses. To examine the contribution of membrane anchorage to the maintenance of the metastable pretriggered Env conformation, we compared wild-type and State-1-stabilized Envs solubilized in detergents or in styrene-maleic acid (SMA) copolymers. SMA directly incorporates membrane lipids and resident membrane proteins into lipid nanodiscs (SMALPs). The integrity of the Env trimer in SMALPs was maintained at both 4°C and room temperature. By contrast, Envs solubilized in Cymal-5, a non-ionic detergent, were unstable at room temperature, although their stability was improved at 4°C and after incubation with the entry inhibitor BMS-806. Envs solubilized in ionic detergents were relatively unstable at either temperature. Comparison of Envs solubilized in Cymal-5 and SMA at 4°C revealed subtle differences in bNAb binding to the gp41 membrane-proximal external region (MPER), consistent with these distinct modes of Env solubilization. Otherwise, the antigenicity of the Cymal-5- and SMA-solubilized Envs was remarkably similar, both in the absence and presence of BMS-806. However, both solubilized Envs were recognized differently from the mature membrane Env by specific bNAbs and pNAbs. Thus, detergent-based and detergent-free solubilization at 4°C alters the pretriggered membrane Env conformation in

consistent ways, indicating that loss of Env association with the membrane results in default state(s).

IMPORTANCE

The human immunodeficiency virus (HIV-1) envelope glycoproteins (Envs) in the viral membrane mediate virus entry into the host cell and are targeted by neutralizing antibodies elicited by natural infection or vaccines. Detailed studies of membrane proteins rely on purification procedures that allow the proteins to maintain their natural conformation. In this study, we show that a styrene-maleic acid (SMA) copolymer can extract HIV-1 Env from a membrane without the use of detergents. The Env in SMA is more stable at room temperature than Env in detergents. The purified Env in SMA maintains many but not all of the characteristics expected of the natural membrane Env. Our results underscore the importance of the membrane environment to the native conformation of HIV-1 Env. Purification methods that bypass the need for detergents could be useful tools for future studies of HIV-1 Env structure and its interaction with receptors and antibodies.

KEYWORDS

Virus, membrane, Env, solubilization, Cymal-5, DIBMA, SMA, default conformation, structure, detergent

INTRODUCTION

Human immunodeficiency virus (HIV-1) entry is mediated by the envelope glycoprotein (Env) trimer, a Class I viral fusion protein composed of three gp120 exterior subunits and three gp41 transmembrane subunits (1-3). In HIV-1 infected cells, Env is synthesized in the endoplasmic reticulum as an ~856-amino acid precursor that trimerizes and undergoes signal peptide cleavage and the addition of high-mannose glycans (4-7). In the Golgi compartment, the gp160 Env precursor is cleaved by host furin-like proteases into the gp120 and gp41 subunits and is further modified by the addition of complex carbohydrates (8-12). These mature Envs are selectively incorporated into virions (8).

Single-molecule fluorescence resonance energy transfer (smFRET) experiments indicate that, on virus particles, the Env trimer exists in three conformational states (States 1 to 3) (13). The metastable pretriggered Env conformation (State 1) predominates on virions from primary HIV-1 strains; upon interaction with the receptors, CD4 and CCR5 or CXCR4, Env undergoes transitions to lower-energy states (States 2 and 3) (13-15). Receptor-induced transitions in gp41 result in the interaction of the N-terminal fusion peptide with the target cell membrane and in the formation of a six-helix bundle that drives the fusion of viral and cell membranes (16-24).

In natural HIV-1 infection, Env strain variability, heavy glycosylation and conformational flexibility contribute to HIV-1 persistence by diminishing the binding and elicitation of neutralizing antibodies (25-29). The gp160 Env precursor, which samples

multiple conformations, and disassembled Envs (shed gp120, gp41 six-helix bundles) elicit high titers of poorly neutralizing antibodies (pNAbs) that fail to recognize the mature pretriggered (State-1) Env trimer (30-35). After years of infection, a minority of HIV-1-infected individuals generate broadly neutralizing antibodies (bNAbs), most of which recognize the cleaved pretriggered (State-1) Env conformation (13, 36-43). Six categories of bNAbs that target different Env epitopes have been identified (Table 1) (27,29,44,45). Although passively administered monoclonal bNAbs are protective in animal models of HIV-1 infection (46-49), suggesting their potential utility in prophylaxis, bNAbs have not been efficiently and consistently elicited by current vaccine candidates (50-54).

Differences in the antigenicity, glycosylation and conformation of soluble Env trimers used as immunogens and the pretriggered (State-1) membrane Env have been observed (12,55-59). Given the requirement for bNAbs to recognize conserved, conformation-specific and often glycan-dependent elements on the pretriggered (State-1) Env (13,36-43), even small differences from the native State-1 Env might affect immunogen efficacy. Both the conformation and the glycan composition of the State-1 Env depend upon association with the membrane (12,57,60-65). These considerations recommend the need to study HIV-1 Envs in native membrane environments.

In preparation for their biochemical, biophysical and structural characterization, membrane proteins are often solubilized in detergents to allow purification. In some cases, the purified proteins can be reconstituted into a phospholipid membrane

environment such as proteoliposomes or nanodiscs (66,67). For metastable membrane proteins such as HIV-1 Env, detergent solubilization could lead to irreversible effects on conformation. Indeed, Env conformations resembling State 2, which has been suggested to represent a default conformation (68,69), have been observed for detergent-solubilized HIV-1 Envs, including those reconstituted into proteoliposomes or nanodiscs (58,70-73). To allow membrane protein purification and characterization while bypassing completely the need for detergent solubilization, styrene-maleic acid (SMA) copolymers have been developed that directly solubilize lipid membranes and resident membrane proteins into 9-15-nm discoidal nanoparticles (SMA lipid particles or SMALPs) (74-80). In some cases, membrane proteins in SMALPs have been shown to be thermostable compared to the detergent-solubilized proteins (80,81). The cryo-electron microscopy (cryo-EM) structure of the multidrug exporter AcrB in SMALPs revealed a remarkably well-ordered lipid bilayer associated with the transmembrane domains of the protein (82). Here, we compare the stability and antigenicity of HIV-1 Envs solubilized using SMA versus detergents (Cymal-5 or SDS/deoxycholate). Such studies provide insights into the important contribution of protein-membrane interactions to the maintenance of a native Env conformation.

RESULTS

Antigenicity of a State-1-stabilized HIV-1_{AD8} Env variant on the surface of expressing cells. A previous study described HIV-1_{AD8} Env mutants with increased State-1 stability, improved precursor cleavage, and a higher content of lysine residues potentially useful for crosslinking (83). One of these HIV-1_{AD8} variants, 2-4 RM6 E, will

be used throughout this study and, in some cases, will be compared with the wild-type (wt) HIV-1_{AD8} Env (see Material and Methods for a more detailed description of these Envs). To provide a standard for the antigenicity of a native, State-1-enriched membrane Env, we evaluated the recognition of cleaved and uncleaved 2-4 RM6 E Env on the surface of expressing A549 cells by panels of pNAbs and bNAbs (Fig. 1, Table 1). As expected (43, 71), the pNAbs preferentially recognized the 2-4 RM6 E gp160 Env but not the cleaved gp120 and gp41 Envs. By contrast, the bNAbs precipitated the cleaved gp120 and gp41 Envs, indicating their ability to bind the mature Env trimer on the cell surface. The antigenicity profile of the cell-surface 2-4 RM6 E Env is similar to that previously reported for the wt HIV-1_{AD8} Env (43).

Antigenicity of wt and 2-4 RM6 E Envs in a cell membrane preparation. Preparation of cell membranes is often used as an initial step in the purification of membrane proteins, as cell nuclei, mitochondria and cytosolic proteins are removed. To evaluate the potential effect of membrane preparation on Env conformation, we examined the antigenicity of the wt HIV-1_{AD8} and the 2-4 RM6 E Envs in membranes purified from expressing A549 cells (Fig. 2). We evaluated membrane Env antigenicity in the absence and presence of BMS-806, a small-molecule HIV-1 entry inhibitor that decreases Env transitions from State 1 and thereby stabilizes the pretriggered conformation (13,43,59,84-86). Briefly, after incubation with a panel of pNAbs and bNAbs, the purified cell membranes were lysed in an NP-40 buffer and the Env-antibody complexes were captured on Protein A-Sepharose beads and analyzed by Western blotting. The 2-4 RM6 E Env was proteolytically processed more efficiently than the wt HIV-1_{AD8} Env, as

178 expected (83), resulting in a relative increase in the cleaved 2-4 RM6 E Env in the Input
179 samples (Fig. 2A). Most pNAbs efficiently recognized the wt and 2-4 RM6 E gp160
180 Envs. The addition of BMS-806 slightly reduced gp160 binding by the F105 pNAb
181 against the CD4 binding site and the 17b pNAb against a CD4-induced (CD4i) gp120
182 epitope; both epitopes are near the BMS-806 binding site (87). Recognition of the
183 cleaved Envs by the pNAbs was generally inefficient; however, the 19b anti-V3 pNAb
184 and to a lesser extent the 17b CD4i pNAb recognized the wt and 2-4 RM6 E gp120
185 glycoproteins. This binding of the 19b and 17b pNAbs to gp120 was inhibited by BMS-
186 806; moreover, when normalized to the Input gp120, the recognition of the 2-4 RM6 E
187 gp120 by the 19b and 17b pNAbs was reduced compared with that of the wt HIV-1_{AD8}
188 Env (Fig. 2B, left panels). These observations suggest that the exposure of V3 and
189 CD4i epitopes may result from the spontaneous sampling of more open State 2/3-like
190 conformations by the Envs on the purified cell membranes. Spontaneous exposure of
191 gp120 V3 and CD4i epitopes on intact HIV-1_{AD8} virions has recently been observed (88)
192 and is consistent with the conformational flexibility of virion Envs documented by
193 smFRET studies (13,59,85). Two representative bNAbs, PGT121 against a V3-glycan
194 epitope and PGT145 against the trimer apex, recognized the cleaved wt and 2-4 RM6 E
195 Envs efficiently in the absence or presence of BMS-806. Thus, the antibody binding
196 profiles of the wt HIV-1_{AD8} and 2-4 RM6 E Envs in the purified membranes correspond
197 to those observed for these Envs on the cell and viral surfaces (Fig.1 and references 43
198 and 88).
199

Comparison of the ability of different amphipathic copolymers to extract HIV-1 Env from membranes. Although SMALPs have proven to be of great utility for membrane protein solubilization and characterization (74-82), they do have limitations. SMALPs need to be maintained at low concentrations of divalent cations and at pH values above 7.5 to remain in solution (77,80). Likely due to the aromatic styrene groups in the SMA copolymer, SMALPs absorb ultraviolet light, interfering with protein concentration measurements at 280 nm (77). Efforts have been made to overcome these limitations by replacing maleic acid with other hydrophilic moieties (e.g., glycerol, glucosamine) or supplanting styrene with diisobutyrene (Fig. 3) (89,90).

We compared commercially available preparations of SMA and diisobutyrene-maleic acid (DIBMA) variants with an in-house preparation of SMA (see Materials and Methods). The efficiency with which these amphipathic copolymers extracted a crosslinked, State-1-stabilized Env, AE.2, from cell membranes was compared. The AE.2 Env is closely related to the 2-4 RM6 E Env, but has one additional State-1-stabilizing change and one additional lysine substitution for potential crosslinking (see Materials and Methods) (83). Cell membranes prepared from A549 cells expressing the His_6-tagged AE.2 Env were crosslinked with DTSSP. The crosslinked membrane was divided into equal parts, which were used for the extraction of Env by the different amphipathic copolymers. The solubilized Envs were purified on Ni-NTA beads and subjected to SDS-PAGE and silver staining (Fig. 4A). The highest yield of Env was obtained with our in-house SMA, with slightly lower Env yields obtained with DIBMA 10, DIBMA 12 and SMA 11001. The SMA 11001, which unlike the other SMA variants has a

dimethylaminopropylamine (DMAPA) group, extracted a higher proportion of uncleaved gp160 and crosslinked gp120-gp41 Env than the other SMA copolymers. These results indicate that the ratio and the nature of the hydrophobic and polar groups in the copolymer can influence the yield and maturity of the extracted Envs.

We next examined the antigenic profiles of the crosslinked and purified AE.2 Envs extracted with the different amphipathic copolymers. The ability of four bNAbs (2G12, PGT145, PG9 and VRC03) and the 19b pNAb to recognize the solubilized AE.2 Envs was evaluated. PGT145, PG9 and VRC03 exhibit some preference for State-1 Envs; 2G12 recognizes gp120 outer domain glycans in a manner that is less dependent on the Env conformational state (13,43,68,69). Also, PGT145 and PG9 preferentially recognize cleaved Envs (13,68,69,91). Differences in the yield of Env influenced the amounts of Env precipitated by the antibodies (Fig. 4B). For the instances where bNAb recognition was detectable, the overall pattern of bNAb recognition was similar for all copolymers. The 2G12 bNAb recognized most of the solubilized Envs in proportion to the yields. On the other hand, recognition of the purified AE.2 Envs by the State-1 preferring bNAbs was relatively weak, indicating that the pretriggered Env conformation was only inefficiently preserved in the amphipathic copolymer complexes. With the exception of the uncleaved AE.2 Env extracted by SMALP 11001, the purified AE.2 Envs were inefficiently recognized by the 19b pNAb. As the yield of antigenically similar, cleaved Env trimers extracted by our in-house SMA was at least as good as that of any of the other copolymers, we used our in-house SMA for the following studies.

Stability of solubilized Env trimers at different temperatures. Some membrane proteins in SMALPs or DIBMA nanodiscs have been suggested to be more stable than when solubilized in detergents (79,81,82,92-94). We compared the stability of the wt HIV-1_{AD8} and 2-4 RM6 E Env trimers solubilized in Cymal-5 (a nonionic detergent), SMA and RIPA buffer (which contains two ionic detergents, SDS and deoxycholate). Both Envs were extracted from expressing cells slightly more efficiently by Cymal-5 and RIPA than by SMA (see Input in Fig. 5A). To evaluate the stability of the solubilized Envs, we took advantage of the His_6 tag at the gp41 C-terminus, which allows the Envs to be precipitated using Ni-NTA beads. The ratio of the gp120:gp160 Envs in the precipitated samples provides an indication of the stability of the Env trimer in solution (43). In this manner, Env trimer stability was measured at either 4°C or room temperature for 1 and 16 h (Fig. 5A and B). Under all conditions tested, the wt and 2-4 RM6 E Envs were less stable in RIPA buffer than in Cymal-5 or SMA. The addition of BMS-806 during the solubilization only minimally improved the stability of the Envs in RIPA buffer; the positive effect of BMS-806 on RIPA-solubilized Envs was observed only during the 1-h experiment at 4°C. Apparently, the instability of the RIPA-solubilized Env trimers at room temperature or for longer incubation periods precluded the possibility of detecting a stabilizing effect of BMS-806.

The wt and 2-4 RM6 E Envs solubilized in SMA or Cymal-5 exhibited comparable stability during a 1-h incubation at 4°C in the absence of BMS-806; the stability of both Envs solubilized in Cymal-5 but not in SMA was enhanced by BMS-806 during a long (16-h) incubation at 4°C. Notably, at room temperature in the absence of BMS-806, both

the wt and 2-4 RM6 E Envs in SMALPs were more stable than these Envs in Cymal-5 or RIPA buffer. The addition of BMS-806 did not significantly increase the stability of Envs in SMALPs at either temperature. Blue Native gel analysis revealed that at room temperature, the 2-4 RM6 E Env in SMALPs largely comprises higher-order oligomers consistent with trimers, whereas a substantial fraction of the 2-4 RM6 E Env in Cymal-5 consists of lower-molecular-weight forms (Fig. 6). Thus, compared with detergent-solubilized Envs, Envs in SMALPs maintained better trimer integrity during room temperature incubation.

Antibody binding profile of the 2-4 RM6 E Env in Cymal-5 or SMALPs. The above observations indicate that solubilization in SMA and detergents can exert different effects on the stability of the Env trimers, raising the possibility that solubilization could influence Env antigenicity. To examine this possibility, lysates of A549 cells expressing the 2-4 RM6 E Env were prepared using 1% Cymal-5 or 1% SMA. Initially, we attempted to precipitate the solubilized Env from these cell lysates, but found that the presence of uncomplexed SMA in the lysates non-specifically interfered with immunoprecipitation by all antibodies tested (data not shown). This problem was remedied by partially purifying the 2-4 RM6 E Env in the cell lysates using Ni-NTA beads. After eluting the 2-4 RM6 E Env from the Ni-NTA beads, the antigenicity of the solubilized Env was evaluated by immunoprecipitation by a panel of pNAbs and bNAbs (Fig. 7A and B). In parallel experiments, BMS-806 was added to the cells prior to lysis and maintained in the cell lysates during the initial stage of immunoprecipitation.

In the absence of BMS-806, the cleaved 2-4 RM6 E Env in Cymal-5 was precipitated by all the bNAbs, although relatively weakly by the PGT145, PG16 and VRC03 bNAbs. Precipitation of the cleaved 2-4 RM6 E Env in SMALPs by bNAbs was generally weaker than that seen in Cymal-5, but showed a qualitatively similar pattern. Both Cymal-5- and SMA-solubilized cleaved 2-4 RM6 E Envs were recognized by the 19b and F105 pNAbs and, for the SMA-solubilized Envs, by the 17b pNAb as well. Both solubilized Envs contained populations that apparently shed gp120 and were precipitated by the F240 pNAb, which recognizes a Cluster I epitope on the gp41 ectodomain (95). These observations indicate that the conformations of both Cymal-5- and SMA-solubilized cleaved 2-4 RM6 E Envs differ from that of the cleaved cell-surface or membrane 2-4 RM6 E Env. In particular, the conformational differences between the solubilized cleaved Envs and the membrane cleaved Env are manifest in weaker recognition of the former Envs by the State-1-preferring PGT145, PG9 and VRC03 bNAbs and stronger recognition by V3, CD4BS and CD4i pNAbs. Thus, without BMS-806, the 2-4 RM6 E Env in Cymal-5 micelles or SMALPs readily samples conformations other than State 1.

It is noteworthy that in the absence of BMS-806, the antigenic profiles of the cleaved 2-4 RM6 E Envs solubilized in Cymal-5- and SMA are well correlated (Fig. 8A). The most significant differences between these solubilized Envs relate to recognition by the 4E10 and 10E8 bNAbs against the membrane-proximal external region (MPER) of gp41 (Fig. 8A); such differences may result from local changes in MPER structure associated with the distinct modes of Env solubilization employed by Cymal-5 and SMA.

Recognition of other epitopes on the Cymal-5- and SMA-solubilized Envs was strongly correlated (Fig. 8B). Thus, in the absence of BMS-806 or other ligands, different means of solubilizing the 2-4 RM6 E Env result in similar conformational states.

The addition of BMS-806 changed the antigenic profile of the cleaved 2-4 RM6 E Env in Cymal-5 and SMALPs (Fig. 7A and B). Recognition of the cleaved 2-4 RM6 E Env by the PG16, PGT151 and 35O22 bNAbs (and by the PGT145 bNAb in the case of SMA) was increased in the presence of BMS-806. Recognition of the cleaved Env in Cymal-5 and SMALPs by the 19b, F105, 17b and F240 pNAbs was decreased by BMS-806. Thus, both forms of solubilized Env demonstrated an antigenic profile closer to that of the cell-surface Env when BMS-806 was present. Nonetheless, the relatively weak binding of the PGT145 and VRC03 bNAbs and the residual binding of the 19b and F105 pNAbs to the cleaved 2-4 RM6 E Env in Cymal-5 and SMALPs indicate conformational differences from the mature membrane Env. Similar to our observation in the absence of BMS-806 (Fig. 8A), we observed that the antigenic profiles of the Cymal-5- and SMA-solubilized 2-4 RM6 E Envs correlated in the presence of BMS-806 (Fig. 8C). Apparently, distinct modalities that extract Env from its membrane environment generate BMS-806-bound Envs in similar, non-State-1 conformations.

As expected (33,43,71), the uncleaved gp160 forms of both Cymal-5 and SMA-solubilized 2-4 RM6 E Envs were recognized efficiently by the pNAbs.

Effect of crosslinking on the antigenicity of Env in SMALPs. The above study suggests that the 2-4 RM6 E Env in SMALPs samples conformations different from those associated with the membrane Env. Crosslinking has been shown to reduce HIV-1 Env conformational flexibility, decreasing the exposure of pNAb epitopes (33,37,71,88,96). We hypothesized that crosslinking the HIV-1 Env in the presence of BMS-806 prior to extraction from the membrane would help to preserve a pretriggered (State-1) conformation after solubilization in SMA. As the 2-4 RM6 E Env is lysine-rich (83), we chose the lysine-specific crosslinker, DTSSP. DTSSP crosslinks are able to be reduced, allowing crosslinked gp120 and gp41 subunits to be distinguished from uncleaved gp160 on Western blots. Membranes prepared from A549 cells expressing the 2-4 RM6 E Env were crosslinked with DTSSP in the presence of BMS-806. BMS-806-treated control membranes were mock treated without crosslinker in parallel. The membranes were solubilized with SMA and the 2-4 RM6 E Env was purified on Ni-NTA beads. After elution of Env, the binding of antibodies was studied by immunoprecipitation, as described above.

DTSSP crosslinking of the 2-4 RM6 E Env reduced recognition of the cleaved Env by the 19b anti-V3 pNAb, and decreased binding of the 19b and F240 pNAbs to the uncleaved gp160 Env (Fig. 9). The binding of bNAbs to the cleaved 2-4 RM6 E Env was not significantly affected by DTSSP treatment. The relatively inefficient recognition of the 2-4 RM6 E Env in SMALPs by the PGT145 and VRC03 bNAbs was not improved by DTSSP crosslinking prior to solubilization. These observations suggest that crosslinking may be useful in reducing the exposure of some pNAb epitopes that accompanies Env

360 solubilization in SMA. However, crosslinking did not prevent the Env conformational
361 changes associated with extraction into SMALPs that diminish recognition by the State-
362 1-preferring PGT145 and VRC03 bNAbs.
363
364 **Effect of pNAb counterselection on 2-4 RM6 E Env antigenicity.** As the uncleaved
365 Env is conformationally flexible and not functional (8,33-35,43,71), its removal from
366 HIV-1 Env preparations would be desirable. The 19b V3-directed pNAb and the F240
367 pNAb against the gp41 ectodomain efficiently recognized the uncleaved Env (Fig. 10A).
368 We tested whether the uncleaved gp160 Env could be preferentially removed from the
369 2-4 RM6 E Env preparation by counterselection with these pNAbs (97). Membranes
370 from BMS-806-treated 2-4 RM6 E Env-expressing cells were crosslinked with DTSSP
371 and used for the preparation of Env-SMALPs. After purification on Ni-NTA beads, the
372 eluted Env-SMALPs were incubated with 19b and F240 pNAbs and Protein A-
373 Sepharose beads. The antigenic profile of the 19b/F240-counterselected 2-4 RM6 E
374 Env was evaluated as described above. Counterselection with the 19b and F240 pNAbs
375 reduced the relative ratio of gp160:gp120 in the preparation (compare Input samples in
376 Fig. 10A and B). The counterselected cleaved 2-4 RM6 E Env preparation was
377 recognized by most of the bNAbs, except for the PGT145 bNAb against the V2
378 quaternary epitope at the trimer apex and the VRC03 CD4BS antibody (Fig. 10B). The
379 recognition of the uncleaved gp160 by pNAbs was very inefficient following 19b/F240
380 counterselection. These results indicate that pNAb counterselection of BMS-
381 806/DTSSP-treated Env-SMALPs can enrich the cleaved Env, which remains
382 accessible to most bNAbs and less accessible to pNAbs.

DISCUSSION

The metastability of the pretriggered (State-1) Env conformation, which is of great interest as a target for small-molecule virus entry inhibitors and vaccine-elicited antibodies, creates challenges for its purification and characterization. The cleaved Env in cell membranes exhibits an antigenic profile that strongly correlates with HIV-1 sensitivity to neutralization (43,71). This observation suggests that the cleaved cell membrane Env closely approximates the functional pretriggered (State-1) Env conformation on the virion. In this study, we take several approaches to address the challenges for HIV-1 Env purification created by the requirement that Env must be extracted from its native membrane environment. Several studies characterizing phenotypes of HIV-1 Envs with alterations in the membrane-proximal external region (MPER) of gp41 have suggested a dependence of the State-1 conformation on Env association with the membrane (60-65). We evaluated the consequences of extracting HIV-1 Env from membranes on the level of cleavage, trimer integrity and antigenicity. In solubilizing Env, we took measures that, in the case of other integral membrane proteins, minimize conformational disruption (74-81,89,90,92,93). In addition to using a lysine-rich, State-1-stabilized Env variant treated with BMS-806 and a crosslinker, we explored the use of amphipathic copolymers that bypass the need for detergents, solubilizing membrane proteins directly in nanodiscs.

SMA efficiently extracted HIV-1 Env from cell membranes. The stability of Env trimers in SMALPs, particularly at room temperature, was superior to that in Cymal-5 or

406 SDS/deoxycholate. Even without the State-1-stabilizing entry inhibitor, BMS-806, HIV-1
407 Env-SMALPs maintained subunit association for over 16 hours at room temperature.
408 The stability of these amphipathic copolymer-Env complexes may be useful in the
409 establishment of cell-free models of Env function or in tests of Env immunogenicity.
410
411 Our antigenicity analyses revealed differences between the 2-4 RM6 E Env in
412 cell membranes and the Envs solubilized in SMA or Cymal-5. In the absence of BMS-
413 806, V3, CD4BS and CD4i pNAb epitopes are exposed in the Env-SMALPs and in
414 Cymal-5-solubilized Env, indicating sampling of non-State-1 conformations. Without
415 BMS-806, recognition of the quaternary V2 epitope at the trimer apex by PGT145 and
416 the VRC03 CD4BS epitope was relatively inefficient for the Cymal-5-solubilized Env and
417 Env-SMALPs. As the PGT145 and VRC03 bNAbs demonstrate some preference for the
418 functional State-1 conformation (68,69), weak recognition of these solubilized Envs is
419 consistent with disruption of the State-1 conformation. The conformational effects
420 associated with extraction of the 2-4 RM6 E Env from membranes could be partially but
421 not completely mitigated by pre-treatment of the membrane Env with BMS-806 and a
422 crosslinker. Treatment of the membrane 2-4 RM6 E Env with BMS-806 and DTSSP
423 decreased the exposure of pNAb epitopes in the Env-SMALPs and enhanced
424 recognition by some, but not all, bNAbs. In particular, PGT145 and VRC03 binding was
425 still weak, suggesting that the 2-4 RM6 E Env in the BMS-806/DTSSP-treated Env-
426 SMALPs assumes a conformation that resembles, but is still distinct from, State 1.
427

What conformations are assumed by the solubilized Envs in Cymal-5 micelles or SMALPs? Subtle differences between these solubilized Env complexes were detected in the gp41 MPER. The 4E10 and 10E8 bNAbs against the gp41 MPER recognized the Cymal-5-solubilized 2-4 RM6 E Env more efficiently than the SMA-solubilized Env, in the absence of BMS-806. Differential recognition by these antibodies presumably reflects structural differences in the MPER associated with these distinct methods of Env solubilization. Other than these differences in recognition by MPER-directed bNAbs, the antigenicity of the Cymal-5-solubilized and SMA-solubilized 2-4 RM6 E Envs was similar. The correlation between the antigenic profiles of the 2-4 RM6 E Env solubilized in Cymal-5 and SMA indicates that membrane extraction without BMS-806 results in similar non-State-1 Env conformations in these two preparations (Fig. 11). Of interest, State 2 has been suggested to represent a default intermediate conformation assumed when the State-1 conformation of the membrane Env is disrupted (68,69). Env solubilization may likewise consign Env to a default conformation resembling State 2, a model consistent with the smFRET profile of a Cymal-5-solubilized uncleaved Env (71). Very recent cryo-EM structures of cleaved HIV-1 Envs in SMALPs reveal asymmetric trimers (98); the distinct pattern of opening angles among the protomers resembles that seen for the uncleaved Env solubilized in Cymal-5 and amphipol A8-35 (71). These structures represent reasonable candidates for the default State-2 Env conformation that, at least upon binding CD4, is thought to be asymmetric (99). The Env-SMALP structures suggest that State 1-to-State 2 transitions may involve breaking trimer symmetry coupled with trimer tilting in the membrane (98). Together, these observations support a model in which disruption of the metastable symmetric State-1 conformation

by Env solubilization and loss of membrane interactions leads to an asymmetric trimer in the default intermediate (State-2) conformation. Changes in Env structure that are coupled to the breaking of symmetry result in the stabilization of State-2 (98), explaining the difficulty of reverting State 2 to State 1 in the absence of a membrane (59,85).

A more complete understanding of the differences between State 1 and State 2 could assist the design of small-molecule entry inhibitors that prematurely activate or block Env transitions between these conformations (84-87,100). The antigenic differences that we identified between the solubilized cleaved Envs (potentially in State-2-like conformations) and the cleaved membrane Env (mostly in a State-1 conformation) may affect the efficacy of vaccine immunogens. A recent antigenicity analysis has suggested that only modest differences exist between the State-1 and State-2 Env conformations, although failure to distinguish cleaved and uncleaved Envs in that study may have diminished the ability of some of the antibodies to discriminate between these conformations (100). The results reported herein will guide future efforts to stabilize the State-1 Env further and to improve methods to solubilize HIV-1 Env with minimal conformational disruption.

MATERIALS AND METHODS

HIV-1 Env constructs. The wild-type (wt) HIV-1_{AD8}, 2-4 RM6 E and AE.2 Envs were coexpressed with the Rev protein, using the natural arrangement of HIV-1 *env* and *rev* sequences (60,83). The Asp 718 (Kpn I) – Bam HI *env* fragments encoding the above Envs were inserted into the corresponding sites of the pSVIIIenv plasmid expressing the

474 HIV-1_{HXBc2} Env and Rev. Thus, these Envs contain a signal peptide and part of the
475 cytoplasmic tail from the HIV-1_{HXBc2} Env. A GGGHHHHHH (His_6) tag was added to the
476 carboxyl terminus of all three Envs. Compared with the HIV-1_{AD8} Env, the 2-4 RM6 E
477 Env has two State-1-stabilizing changes, Q114E and Q567K, and several additional
478 lysine substitutions to improve crosslinking efficiency (R166K, R178K, R315K, R419K,
479 R557K, R633K, Q658K, A667K and N677K) (83). Compared with the 2-4 RM6 E Env,
480 the AE.2 Env has one additional State-1-stabilizing change, A582T, and an additional
481 lysine substitution, R252K (83).
482
483 **SMA and DIBMA.** SMA (2:1) was purchased from Cray Valley and hydrolyzed as
484 described (77). SMA and DIBMA variants were purchased from Cube Biotech.
485
486 **Reagents.** BMS-378806 (herein called BMS-806) was purchased from Selleckchem.
487 Cymal-5 and Cymal-6 were purchased from Anatrace, RIPA buffer from ThermoFisher
488 and Superflow Ni-NTA from Bio-Rad.
489
490 **Expression of HIV-1 Envs.** Human A549 cells inducibly expressing the wt HIV-1_{AD8}
491 Env, the 2-4 RM6 E Env and the AE.2 Env were established as described (43). A549
492 cells constitutively expressing the reverse tet transactivator (rtTA) were transduced with
493 HIV-1-based lentivirus vectors expressing Rev and the above Envs. The vector
494 transcribes a bicistronic mRNA comprising *rev* and *env* and two selectable marker
495 genes (puromycin-T2A-enhanced green fluorescent protein (EGFP)) fused in-frame with
496 a T2A peptide-coding sequence. In the transduced cells, Env expression is controlled

by the Tet-Responsive Element (TRE) promoter and tet-on transcriptional regulatory elements. Env expression is induced by treating the cells with 2 ug/ml doxycycline. The Env-expressing cells were enriched by fluorescence-activated cell sorting for the co-expressed EGFP marker. These polyclonal A549 cell lines were used as sources of Env for the studies reported herein.

Cell lines. The A549 cells inducibly expressing the wt HIV-1_{AD8}, 2-4 RM6 E and AE.2 Envs were grown in DMEM/F12 supplemented with 10% FBS, L-glutamine and penicillin-streptomycin. All cell culture reagents are from Life Technologies.

Antibodies. Antibodies against HIV-1 Env were kindly supplied by Dr. Dennis Burton (Scripps), Drs. Peter Kwong and John Mascola (Vaccine Research Center, NIH), Dr. Barton Haynes (Duke), Dr. Hermann Katinger (Polymun), Dr. James Robinson (Tulane) and Dr. Marshall Posner (Mount Sinai Medical Center). In some cases, anti-Env antibodies were obtained through the NIH AIDS Reagent Program. Antibodies for Western blotting include goat anti-gp120 polyclonal antibody (ThermoFisher) and the 4E10 human anti-gp41 antibody (Polymun). An HRP-conjugated goat anti-human IgG (Santa Cruz) and an HRP-conjugated goat anti-rabbit antibody (Santa Cruz) were used as secondary antibodies for Western blotting.

Immunoprecipitation of cell-surface HIV-1 Env. Doxycycline-induced A549-Env cells were washed twice with washing buffer (1x PBS + 5% FBS). The cells were then incubated with 5 µg/ml antibody for one hour at 4°C. After washing four times in

washing buffer, the cells were lysed in NP-40 lysis buffer (1% NP-40, 0.5 M NaCl, 10 mM Tris, pH 7.5) for five minutes on ice. The lysates were cleared by centrifugation at 13,200 x g for 10 minutes at 4°C, and the clarified supernatants were incubated with Protein A-Sepharose beads for one hour at room temperature. The beads were pelleted (1,000 rpm x 1 min) and washed three times with wash buffer (20 mM Tris-HCl (pH 8.0), 100 mM $(NH_4)_2SO_4$, 1 M NaCl and 0.5% NP-40). The beads were suspended in 2x lithium dodecyl sulfate (LDS) sample buffer, boiled and analyzed by Western blotting using 1:2000 goat anti-gp120 polyclonal antibody (ThermoFisher) and 1:2000 HRP-conjugated rabbit anti-goat IgG (ThermoFisher). The HIV-1 gp41 Env was analyzed by Western blotting with the 4E10 anti-gp41 antibody and HRP-conjugated goat anti-human IgG (Santa Cruz).

For analysis of total Env expression in the cells, clarified cell lysates were prepared from cells that were induced with doxycycline but not incubated with antibodies. The clarified cell lysates were analyzed by Western blotting as described above and serve as the Input samples.

Membrane purification and DTSSP crosslinking. A549 cells expressing the wt HIV-1_{AD8} or 2-4 RM6 E Envs were incubated with 5 mM EDTA in 1x PBS at 37°C until the cells detached from the tissue-culture plates. The cells were pelleted and resuspended in 1x PBS. Cells were spun down at 1500 x g for 10 minutes. The supernatants were removed and homogenization buffer (10 mM Tris HCl (pH 7.5), 250 mM sucrose, 1 mM EDTA, 1x protease inhibitor cocktail) was added to the cell pellet. The cells were

transferred into a glass Dounce homogenizer and homogenized with 250 strokes on ice. The homogenate was spun at 1000 x g for 10 minutes at 4°C. The supernatants were centrifuged at 10,000 x g for 10 minutes at 4°C. The supernatants were spun again at 100,000 x g for 35 minutes at 4°C. The pellet represented the purified membrane fraction.

For DTSSP crosslinking, membranes were washed in 1x PBS and centrifuged at 100,000 g for 25 minutes. Membranes were resuspended in 1x PBS and crosslinked with 0.35 mM DTSSP at 4°C for 45 minutes.

Immunoprecipitation of cell-membrane HIV-1 Envs. Purified cell membranes from Env-expressing A549 cells were incubated with 5 ug/ml antibody for one hour at 4°C, in either the absence or presence of 10 μM BMS-806. The membranes were pelleted at 13,200 x g for 10 minutes at 4°C. The pelleted membranes were lysed in 1% NP-40 with or without BMS-806 for 5 minutes on ice. The membrane lysates were then incubated with Protein A-Sepharose beads for one hour at 4°C. The precipitated proteins were subjected to Western blotting with a goat anti-gp120 antiserum or the human 4E10 anti-gp41 antibody, as described above.

For the Input sample, an aliquot of the cell membrane preparation was lysed in 1% NP-40 and subjected to Western blotting as described above.

Solubilization of Env from membranes. For extraction of Env from membranes, the purified membrane fractions were resuspended in the following buffers:

SMA solubilization buffer (20 mM Tris-HCl, pH 8.0, 100 mM $(NH_4)_2SO_4$, 250 mM NaCl 1% SMA, 1x protease inhibitor cocktail (Roche));

DIBMA solubilization buffer (20 mM Tris-HCl, pH 8.0, 100 mM $(NH_4)_2SO_4$, 250 mM NaCl, 1% DIBMA, 1x protease inhibitor cocktail (Roche));

Cymal-5 solubilization buffer (20 mM Tris-HCl, pH 8.0, 100 mM $(NH_4)_2SO_4$, 250 mM NaCl, 1% Cymal-5, 1x protease inhibitor cocktail (Roche)); and

RIPA buffer (ThermoFisher) (25 mM Tris-HCl, pH 7.6, 150 mM NaCl, 1% NP-40,1% sodium deoxycholate, 0.1% SDS, 1x protease inhibitor cocktail (Roche)).

Solubilized Envs were analyzed on reducing and non-reducing gels. For comparison of SMA and DIBMA variants, gels were silver stained using the Pierce Silver stain kit (Thermo Scientific) or Western blotted as described above.

Solubilization of Env from cells. Env-expressing cells were induced with 2 ug/ml of doxycycline for two days to express HIV-1 Envs and detached by incubating with 5 mM EDTA at 37^{o}C. Cells were aliquoted and lysed with the solubilization buffers described above at either 4^{o}C or room temperature.

Association of gp120 with solubilized Env complexes. The noncovalent association of gp120 with solubilized Env complexes was studied by precipitating the proteins using the carboxy-terminal His_6 tag. Clarified cell lysates were prepared from Env-expressing

A549 cells as described above. Aliquots of the lysates were saved for Western blotting to detect the gp160, gp120 and gp41 glycoproteins in the Input sample. The bulk of the lysates was incubated for 1 h or 16 h at 4°C or room temperature, in some cases in the presence of 10 μM BMS-806. The lysates were then incubated for 1 h with nickel-nitriloacetic acid (Ni-NTA) beads (Qiagen) at the indicated temperatures (4°C or room temperature), in some cases with 10 μM BMS-806. The beads were pelleted (1,000 rpm for 1 min at 4°C or room temperature), washed three times at 4°C or room temperature with wash buffer (20 mM Tris-HCl (pH 8.0), 100 mM $(NH_4)_2SO_4$, 1 M NaCl, 30 mM imidazole), boiled in 2x LDS sample buffer, and analyzed by Western blotting as described above. The association of gp120 with the Env complex for each solubilization buffer was calculated as follows:

$(gp120/gp160)_{precipitated} \div (gp120/gp160)_{Input}$.

Immunoprecipitation of solubilized Envs from cell lysates. A549 cells were induced with doxycycline to express the 2-4 RM6 E Env. Forty-eight hours later, the cells were lysed with either Cymal-5 or SMA solubilization buffer, as described above. The 2-4 RM6 E Env was incubated with Ni-NTA beads at 4°C for 1.5 hours. After incubation, the mixture was applied to an Eco-column (Biorad). The beads were washed with 30 bed volumes of washing buffer (20 mM Tris-HCl (pH 8.0), 100 mM $(NH_4)_2SO_4$, 1 M NaCl, 30 mM imidazole), and eluted with 10 bed volumes of elution buffer (20 mM Tris-HCl (pH 8.0), 100 mM $(NH_4)_2SO_4$, 250 mM NaCl, 250 mM imidazole). The purified Env was aliquoted and incubated with 10 μg/ml antibodies together with Protein A-Sepharose beads for 1 h at 4°C. For the samples with BMS-806, 10 μM BMS-806 was added

before cell lysis and remained in all the following steps. An aliquot without added antibody/beads served as the Input sample. The precipitated proteins and Input sample were Western blotted as described above.

Antigenicity of Envs solubilized from purified membranes. Cell membranes were prepared from A549 cells expressing the 2-4 RM6 E Env as described above. In some cases, the resuspended cell membranes were treated with 0.35 mM DTSSP crosslinker at room temperature for 45 minutes. In some experiments, BMS-806 at 10 µM concentration was added to the membranes at the time of crosslinking. The membranes were then lysed in SMA solubilization buffer containing 10 µM BMS-806 for 30 minutes at room temperature. The 2-4 RM6 E Env was incubated with Ni-NTA beads at 4°C for 1.5 hours. After incubation, the mixture was applied to an Eco-column (Biorad). The Ni-NTA beads were washed with 30 bed volumes of washing buffer (20 mM Tris-HCl (pH 8.0), 100 mM $(NH_4)_2SO_4$, 1 M NaCl, 30 mM imidazole), and eluted with 10 bed volumes of elution buffer (20 mM Tris-HCl (pH 8.0), 100 mM $(NH_4)_2SO_4$, 250 mM NaCl, 250 mM imidazole). For the experiments where counterselection with pNAbs was employed, the purified 2-4 RM6 E Env was incubated with 40 µg/ml of 19b and 40 µg/ml of F240 antibodies and 100 µl of Protein A-Sepharose at room temperature for 30 minutes. The mixture was applied to an Eco-column (Biorad) and the purified 2-4 RM6 E Env was collected in the flow-through.

ACKNOWLEDGMENTS

633 We thank Ms. Elizabeth Carpelan for manuscript preparation. Antibodies against HIV-1
634 were kindly supplied by John C. Kappes (University of Alabama at Birmingham), Dennis
635 Burton (Scripps), Peter Kwong and John Mascola (Vaccine Research Center NIH),
636 Barton Haynes (Duke University), Hermann Katinger (Polymun), James Robinson
637 (Tulane University), and Marshall Posner (Mount Sinai Medical Center). We thank the
638 NIH HIV Reagent Program for providing additional reagents.

639

640 This work was supported by grants from the National Institutes of Health (grant nos.
641 AI 145547, AI 124982, AI 150471, AI 129017 and AI 164562), a grant from Gilead
642 Sciences, and by a gift from the late William F. McCarty-Cooper.

643

644 We declare no conflicts of interest.

645

REFERENCES

1. Wyatt R, Sodroski J. 1998. The HIV-1 envelope glycoproteins: fusogens, antigens, and immunogens. Science 280:1884-8.

2. Chen B. 2019. Molecular mechanism of HIV-1 entry. Trends Microbiol 27:878-891.

3. Harrison SC. 2015. Viral membrane fusion. Virology 479-480:498-507.

4. Willey RL, Bonifacino JS, Potts BJ, Martin MA, Klausner RD. 1988. Biosynthesis, cleavage, and degradation of the human immunodeficiency virus 1 envelope glycoprotein gp160. Proc Natl Acad Sci U S A 85:9580-4.

5. Earl PL, Moss B, Doms RW. 1991. Folding, interaction with GRP78-BiP, assembly, and transport of the human immunodeficiency virus type 1 envelope protein. J Virol 65:2047-55.

6. Pal R, Hoke GM, Sarngadharan MG. 1989. Role of oligosaccharides in the processing and maturation of envelope glycoproteins of human immunodeficiency virus type 1. Proc Natl Acad Sci U S A 86:3384-8.

7. Dewar RL, Vasudevachari MB, Natarajan V, Salzman NP. 1989. Biosynthesis and processing of human immunodeficiency virus type 1 envelope glycoproteins: effects of monensin on glycosylation and transport. J Virol 63:2452-6.

8. Zhang S, Nguyen HT, Ding H, Wang J, Zou S, Liu L, Guha D, Gabuzda D, Ho DD, Kappes JC, Sodroski J. 2021. Dual pathways of human immunodeficiency virus type 1 envelope glycoprotein trafficking modulate the selective exclusion of uncleaved oligomers from virions. J Virol 95:e01369-20.

9. Stein BS, Engleman EG. 1990. Intracellular processing of the gp160 HIV-1 envelope precursor. Endoproteolytic cleavage occurs in a cis or medial compartment of the Golgi complex. J Biol Chem 265:2640-9.

10. Hallenberger S, Bosch V, Angliker H, Shaw E, Klenk HD, Garten W. 1992. Inhibition of furin-mediated cleavage activation of HIV-1 glycoprotein gp160. Nature 360:358-61.

11. Doores KJ, Bonomelli C, Harvey DJ, Vasiljevic S, Dwek RA, Burton DR, Crispin M, Scanlan CN. 2010. Envelope glycans of immunodeficiency virions are almost entirely oligomannose antigens. Proc Natl Acad Sci U S A 107:13800-5.

12. Go EP, Ding H, Zhang S, Ringe RP, Nicely N, Hua D, Steinbock RT, Golabek M, Alin J, Alam SM, Cupo A, Haynes BF, Kappes JC, Moore JP, Sodroski JG, Desaire H. 2017. A glycosylation benchmark profile for HIV-1 envelope

glycoprotein production based on eleven Env trimers. J Virol 91:e02428-16.

13. Munro JB, Gorman J, Ma X, Zhou Z, Arthos J, Burton DR, Koff WC, Courter JR, Smith AB III, Kwong PD, Blanchard SC, Mothes W. 2014. Conformational dynamics of single HIV-1 envelope trimers on the surface of native virions. Science 346:759-63.

14. Wu L, Gerard NP, Wyatt R, Choe H, Parolin C, Ruffing N, Borsetti A, Cardoso AA, Desjardin E, Newman W, Gerard C, Sodroski J. 1996. CD4-induced interaction of primary HIV-1 gp120 glycoproteins with the chemokine receptor CCR-5. Nature 384:179-83.

15. Trkola A, Dragic T, Arthos J, Binley JM, Olson WC, Allaway GP, Cheng-Mayer C, Robinson J, Maddon PJ, Moore JP. 1996. CD4-dependent, antibody-sensitive interactions between HIV-1 and its co-receptor CCR-5. Nature 384:184-7.

16. Khasnis MD, Halkidis K, Bhardwaj A, Root MJ. 2016. Receptor activation of HIV-1 Env leads to asymmetric exposure of the gp41 trimer. PLoS Pathog 12:e1006098.

17. Furuta RA, Wild CT, Weng Y, Weiss CD. 1998. Capture of an early fusion-active conformation of HIV-1 gp41. Nat Struct Biol 5:276-9.

18. Koshiba T, Chan DC. 2003. The prefusogenic intermediate of HIV-1 gp41 contains exposed C-peptide regions. J Biol Chem 278:7573-9.

19. He Y, Vassell R, Zaitseva M, Nguyen N, Yang Z, Weng Y, Weiss CD. 2003. Peptides trap the human immunodeficiency virus type 1 envelope glycoprotein fusion intermediate at two sites. J Virol 77:1666-71.

20. Chan DC, Fass D, Berger JM, Kim PS. 1997. Core structure of gp41 from the HIV envelope glycoprotein. Cell 89:263-73.

21. Weissenhorn W, Dessen A, Harrison SC, Skehel JJ, Wiley DC. 1997. Atomic structure of the ectodomain from HIV-1 gp41. Nature 387:426-30.

22. Lu M, Blacklow SC, Kim PS. 1995. A trimeric structural domain of the HIV-1 transmembrane glycoprotein. Nat Struct Biol 2:1075-82.

23. Melikyan GB, Markosyan RM, Hemmati H, Delmedico MK, Lambert DM, Cohen FS. 2000. Evidence that the transition of HIV-1 gp41 into a six-helix bundle, not the bundle configuration, induces membrane fusion. J Cell Biol 151:413-23.

24. Wilen CB, Tilton JC, Doms RW. 2012. Molecular mechanisms of HIV entry. Adv Exp Med Biol 726:223-42.

738 25. Bonsignori M, Liao HX, Gao F, Williams WB, Alam SM, Montefiori DC, Haynes
739 BF. 2017. Antibody-virus co-evolution in HIV infection: paths for HIV vaccine
740 development. Immunol Rev 275:145-160.
741
742 26. Kwong PD, Mascola JR. 2018. HIV-1 vaccines based on antibody identification,
743 B cell ontogeny, and epitope structure. Immunity 48:855-871.
744
745 27. Sok D, Burton DR. 2018. Recent progress in broadly neutralizing antibodies to
746 HIV. Nat Immunol 19:1179-1188.
747
748 28. Stewart-Jones GB, Soto C, Lemmin T, Chuang GY, Druz A, Kong R, Thomas
749 PV, Wagh K, Zhou T, Behrens AJ, Bylund T, Choi CW, Davison JR, Georgiev IS,
750 Joyce MG, Kwon YD, Pancera M, Taft J, Yang Y, Zhang B, Shivatare SS,
751 Shivatare VS, Lee CC, Wu CY, Bewley CA, Burton DR, Koff WC, Connors M,
752 Crispin M, Baxa U, Korber BT, Wong CH, Mascola JR, Kwong PD. 2016.
753 Trimeric HIV-1-Env structures define glycan shields from Clades A, B, and G.
754 Cell 165:813-26.
755
756 29. Ward AB, Wilson IA. 2017. The HIV-1 envelope glycoprotein structure: nailing
757 down a moving target. Immunol Rev 275:21-32.
758
759 30. Wei X, Decker JM, Wang S, Hui H, Kappes JC, Wu X, Salazar-Gonzalez JF,
760 Salazar MG, Kilby JM, Saag MS, Komarova NL, Nowak MA, Hahn BH, Kwong
761 PD, Shaw GM. 2003. Antibody neutralization and escape by HIV-1. Nature
762 422:307-12.
763
764 31. Labrijn AF, Poignard P, Raja A, Zwick MB, Delgado K, Franti M, Binley J, Vivona
765 V, Grundner C, Huang CC, Venturi M, Petropoulos CJ, Wrin T, Dimitrov DS,
766 Robinson J, Kwong PD, Wyatt RT, Sodroski J, Burton DR. 2003. Access of
767 antibody molecules to the conserved coreceptor binding site on glycoprotein
768 gp120 is sterically restricted on primary human immunodeficiency virus type 1. J
769 Virol 77:10557-65.
770
771 32. Moore PL, Ranchobe N, Lambson BE, Gray ES, Cave E, Abrahams MR,
772 Bandawe G, Mlisana K, Abdool Karim SS, Williamson C, Morris L, Study C,
773 Immunology NCfHAV. 2009. Limited neutralizing antibody specificities drive
774 neutralization escape in early HIV-1 subtype C infection. PLoS Pathog
775 5:e1000598.
776
777 33. Haim H, Salas I, Sodroski J. 2013. Proteolytic processing of the human
778 immunodeficiency virus envelope glycoprotein precursor decreases
779 conformational flexibility. J Virol 87:1884-9.
780
781 34. Pancera M, Wyatt R. 2005. Selective recognition of oligomeric HIV-1 primary
782 isolate envelope glycoproteins by potently neutralizing ligands requires efficient
783 precursor cleavage. Virology 332:145-56.

35. Chakrabarti BK, Pancera M, Phogat S, O'Dell S, McKee K, Guenaga J, Robinson J, Mascola J, Wyatt RT. 2011. HIV type 1 Env precursor cleavage state affects recognition by both neutralizing and nonneutralizing gp41 antibodies. AIDS Res Hum Retroviruses 27:877-87.

36. Guttman M, Cupo A, Julien JP, Sanders RW, Wilson IA, Moore JP, Lee KK. 2015. Antibody potency relates to the ability to recognize the closed, pre-fusion form of HIV Env. Nat Commun 6:6144.

37. Haim H, Salas I, McGee K, Eichelberger N, Winter E, Pacheco B, Sodroski J. 2013. Modeling virus- and antibody-specific factors to predict human immunodeficiency virus neutralization efficiency. Cell Host Microbe 14:547-58.

38. Gray ES, Taylor N, Wycuff D, Moore PL, Tomaras GD, Wibmer CK, Puren A, DeCamp A, Gilbert PB, Wood B, Montefiori DC, Binley JM, Shaw GM, Haynes BF, Mascola JR, Morris L. 2009. Antibody specificities associated with neutralization breadth in plasma from human immunodeficiency virus type 1 subtype C-infected blood donors. J Virol 83:8925-37.

39. Sather DN, Armann J, Ching LK, Mavrantoni A, Sellhorn G, Caldwell Z, Yu X, Wood B, Self S, Kalams S, Stamatatos L. 2009. Factors associated with the development of cross-reactive neutralizing antibodies during human immunodeficiency virus type 1 infection. J Virol 83:757-69.

40. Walker LM, Simek MD, Priddy F, Gach JS, Wagner D, Zwick MB, Phogat SK, Poignard P, Burton DR. 2010. A limited number of antibody specificities mediate broad and potent serum neutralization in selected HIV-1 infected individuals. PLoS Pathog 6:e1001028.

41. Gray ES, Madiga MC, Hermanus T, Moore PL, Wibmer CK, Tumba NL, Werner L, Mlisana K, Sibeko S, Williamson C, Abdool Karim SS, Morris L, Team CS. 2011. The neutralization breadth of HIV-1 develops incrementally over four years and is associated with CD4+ T cell decline and high viral load during acute infection. J Virol 85:4828-40.

42. Hraber P, Seaman MS, Bailer RT, Mascola JR, Montefiori DC, Korber BT. 2014. Prevalence of broadly neutralizing antibody responses during chronic HIV-1 infection. AIDS 28:163-9.

43. Zou S, Zhang S, Gaffney A, Ding H, Lu M, Grover JR, Farrell M, Nguyen HT, Zhao C, Anang S, Zhao M, Mohammadi M, Blanchard SC, Abrams C, Madani N, Mothes W, Kappes JC, Smith AB III, Sodroski J. 2020. Long-acting BMS-378806 analogues stabilize the State-1 conformation of the human immunodeficiency virus type 1 envelope glycoproteins. J Virol 94:e00148-20.

44. McCoy LE, Burton DR. 2017. Identification and specificity of broadly neutralizing antibodies against HIV. Immunol Rev 275:11-20.

45. Haynes BF, Burton DR, Mascola JR. 2019. Multiple roles for HIV broadly neutralizing antibodies. Sci Transl Med 11:eaaz2686.

46. Mascola JR, Lewis MG, Stiegler G, Harris D, VanCott TC, Hayes D, Louder MK, Brown CR, Sapan CV, Frankel SS, Lu Y, Robb ML, Katinger H, Birx DL. 1999. Protection of macaques against pathogenic simian/human immunodeficiency virus 89.6PD by passive transfer of neutralizing antibodies. J Virol 73:4009-18.

47. Mascola JR, Stiegler G, VanCott TC, Katinger H, Carpenter CB, Hanson CE, Beary H, Hayes D, Frankel SS, Birx DL, Lewis MG. 2000. Protection of macaques against vaginal transmission of a pathogenic HIV-1/SIV chimeric virus by passive infusion of neutralizing antibodies. Nat Med 6:207-10.

48. Moldt B, Rakasz EG, Schultz N, Chan-Hui PY, Swiderek K, Weisgrau KL, Piaskowski SM, Bergman Z, Watkins DI, Poignard P, Burton DR. 2012. Highly potent HIV-specific antibody neutralization in vitro translates into effective protection against mucosal SHIV challenge in vivo. Proc Natl Acad Sci U S A 109:18921-5.

49. Parren PW, Marx PA, Hessell AJ, Luckay A, Harouse J, Cheng-Mayer C, Moore JP, Burton DR. 2001. Antibody protects macaques against vaginal challenge with a pathogenic R5 simian/human immunodeficiency virus at serum levels giving complete neutralization in vitro. J Virol 75:8340-7.

50. Pauthner M, Havenar-Daughton C, Sok D, Nkolola JP, Bastidas R, Boopathy AV, Carnathan DG, Chandrashekar A, Cirelli KM, Cottrell CA, Eroshkin AM, Guenaga J, Kaushik K, Kulp DW, Liu J, McCoy LE, Oom AL, Ozorowski G, Post KW, Sharma SK, Steichen JM, de Taeye SW, Tokatlian T, Torrents de la Pena A, Butera ST, LaBranche CC, Montefiori DC, Silvestri G, Wilson IA, Irvine DJ, Sanders RW, Schief WR, Ward AB, Wyatt RT, Barouch DH, Crotty S, Burton DR. 2017. Elicitation of robust Tier 2 neutralizing antibody responses in nonhuman primates by HIV envelope trimer immunization using optimized approaches. Immunity 46:1073-1088 e6.

51. Torrents de la Pena A, de Taeye SW, Sliepen K, LaBranche CC, Burger JA, Schermer EE, Montefiori DC, Moore JP, Klasse PJ, Sanders RW. 2018. Immunogenicity in Rabbits of HIV-1 SOSIP Trimers from Clades A, B, and C, given individually, sequentially, or in combination. J Virol 92:e01957-17.

52. Dubrovskaya V, Tran K, Ozorowski G, Guenaga J, Wilson R, Bale S, Cottrell CA, Turner HL, Seabright G, O'Dell S, Torres JL, Yang L, Feng Y, Leaman DP, Vazquez Bernat N, Liban T, Louder M, McKee K, Bailer RT, Movsesyan A, Doria-Rose NA, Pancera M, Karlsson Hedestam GB, Zwick MB, Crispin M, Mascola

JR, Ward AB, Wyatt RT. 2019. Vaccination with glycan-modified HIV NFL envelope trimer-liposomes elicits broadly neutralizing antibodies to multiple sites of vulnerability. Immunity 51:915-929 e7.

53. Xu K, Acharya P, Kong R, Cheng C, Chuang GY, Liu K, Louder MK, O'Dell S, Rawi R, Sastry M, Shen CH, Zhang B, Zhou T, Asokan M, Bailer RT, Chambers M, Chen X, Choi CW, Dandey VP, Doria-Rose NA, Druz A, Eng ET, Farney SK, Foulds KE, Geng H, Georgiev IS, Gorman J, Hill KR, Jafari AJ, Kwon YD, Lai YT, Lemmin T, McKee K, Ohr TY, Ou L, Peng D, Rowshan AP, Sheng Z, Todd JP, Tsybovsky Y, Viox EG, Wang Y, Wei H, Yang Y, Zhou AF, Chen R, Yang L, Scorpio DG, McDermott AB, Shapiro L, et al. 2018. Epitope-based vaccine design yields fusion peptide-directed antibodies that neutralize diverse strains of HIV-1. Nat Med 24:857-867.

54. Sanders RW, van Gils MJ, Derking R, Sok D, Ketas TJ, Burger JA, Ozorowski G, Cupo A, Simonich C, Goo L, Arendt H, Kim HJ, Lee JH, Pugach P, Williams M, Debnath G, Moldt B, van Breemen MJ, Isik G, Medina-Ramirez M, Back JW, Koff WC, Julien JP, Rakasz EG, Seaman MS, Guttman M, Lee KK, Klasse PJ, LaBranche C, Schief WR, Wilson IA, Overbaugh J, Burton DR, Ward AB, Montefiori DC, Dean H, Moore JP. 2015. HIV-1 VACCINES. HIV-1 neutralizing antibodies induced by native-like envelope trimers. Science 349:aac4223.

55. Alsahafi N, Anand SP, Castillo-Menendez L, Verly MM, Medjahed H, Prevost J, Herschhorn A, Richard J, Schon A, Melillo B, Freire E, Smith AB III, Sodroski J, Finzi A. 2018. SOSIP changes affect human immunodeficiency virus type 1 envelope glycoprotein conformation and CD4 engagement. J Virol 92.

56. Castillo-Menendez LR, Nguyen HT, Sodroski J. 2019. Conformational differences between functional human immunodeficiency virus envelope glycoprotein trimers and stabilized soluble trimers. J Virol 93:e01709-18.

57. Cao L, Pauthner M, Andrabi R, Rantalainen K, Berndsen Z, Diedrich JK, Menis S, Sok D, Bastidas R, Park SR, Delahunty CM, He L, Guenaga J, Wyatt RT, Schief WR, Ward AB, Yates JR, 3rd, Burton DR, Paulson JC. 2018. Differential processing of HIV envelope glycans on the virus and soluble recombinant trimer. Nat Commun 9:3693.

58. Torrents de la Pena A, Rantalainen K, Cottrell CA, Allen JD, van Gils MJ, Torres JL, Crispin M, Sanders RW, Ward AB. 2019. Similarities and differences between native HIV-1 envelope glycoprotein trimers and stabilized soluble trimer mimetics. PLoS Pathog 15:e1007920.

59. Lu M, Ma X, Castillo-Menendez LR, Gorman J, Alsahafi N, Ermel U, Terry DS, Chambers M, Peng D, Zhang B, Zhou T, Reichard N, Wang K, Grover JR, Carman BP, Gardner MR, Nikic-Spiegel I, Sugawara A, Arthos J, Lemke EA, Smith AB III, Farzan M, Abrams C, Munro JB, McDermott AB, Finzi A, Kwong

PD, Blanchard SC, Sodroski JG, Mothes W. 2019. Associating HIV-1 envelope glycoprotein structures with states on the virus observed by smFRET. Nature 568:415-419.

60. Haim H, Strack B, Kassa A, Madani N, Wang L, Courter JR, Princiotto A, McGee K, Pacheco B, Seaman MS, Smith AB III, Sodroski J. 2011. Contribution of intrinsic reactivity of the HIV-1 envelope glycoproteins to CD4-independent infection and global inhibitor sensitivity. PLoS Pathog 7:e1002101.

61. Bradley T, Trama A, Tumba N, Gray E, Lu X, Madani N, Jahanbakhsh F, Eaton A, Xia SM, Parks R, Lloyd KE, Sutherland LL, Scearce RM, Bowman CM, Barnett S, Abdool-Karim SS, Boyd SD, Melillo B, Smith AB III, Sodroski J, Kepler TB, Alam SM, Gao F, Bonsignori M, Liao HX, Moody MA, Montefiori D, Santra S, Morris L, Haynes BF. 2016. Amino acid changes in the HIV-1 gp41 membrane proximal region control virus neutralization sensitivity. EBioMedicine 12:196-207.

62. Ringe R, Bhattacharya J. 2012. Association of enhanced HIV-1 neutralization by a single Y681H substitution in gp41 with increased gp120-CD4 interaction and macrophage infectivity. PLoS One 7:e37157.

63. Blish CA, Nguyen MA, Overbaugh J. 2008. Enhancing exposure of HIV-1 neutralization epitopes through mutations in gp41. PLoS Med 5:e9.

64. Salimi H, Johnson J, Flores MG, Zhang MS, O'Malley Y, Houtman JC, Schlievert PM, Haim H. 2020. The lipid membrane of HIV-1 stabilizes the viral envelope glycoproteins and modulates their sensitivity to antibody neutralization. J Biol Chem 295:348-362.

65. Wang Q, Esnault F, Zhao M, Chiu TJ, Smith AB III, Nguyen HT, Sodroski JG. 2022. Global increases in human immunodeficiency virus neutralization sensitivity due to alterations in the membrane-proximal external region of the envelope glycoprotein can be minimized by distant State 1-stabilizing changes. J Virol 96:e0187821.

66. Hardy D, Bill RM, Jawhari A, Rothnie AJ. 2016. Overcoming bottlenecks in the membrane protein structural biology pipeline. Biochem Soc Trans 44:838-44.

67. Yao X, Fan X, Yan N. 2020. Cryo-EM analysis of a membrane protein embedded in the liposome. Proc Natl Acad Sci U S A 117:18497-18503.

68. Herschhorn A, Ma X, Gu C, Ventura JD, Castillo-Menendez L, Melillo B, Terry DS, Smith AB III, Blanchard SC, Munro JB, Mothes W, Finzi A, Sodroski J. 2016. Release of gp120 restraints leads to an entry-competent intermediate state of the HIV-1 envelope glycoproteins. mBio 7:e01598-16.

69. Herschhorn A, Gu C, Moraca F, Ma X, Farrell M, Smith AB III, Pancera M,

Kwong PD, Schon A, Freire E, Abrams C, Blanchard SC, Mothes W, Sodroski JG. 2017. The beta20-beta21 of gp120 is a regulatory switch for HIV-1 Env conformational transitions. Nat Commun 8:1049.

70. Lee JH, Ozorowski G, Ward AB. 2016. Cryo-EM structure of a native, fully glycosylated, cleaved HIV-1 envelope trimer. Science 351:1043-8.

71. Zhang S, Wang K, Wang WL, Nguyen HT, Chen S, Lu M, Go EP, Ding H, Steinbock RT, Desaire H, Kappes JC, Sodroski J, Mao Y. 2021. Asymmetric structures and conformational plasticity of the uncleaved full-length human immunodeficiency virus envelope glycoprotein trimer. J Virol 95:e0052921.

72. Rantalainen K, Berndsen ZT, Antanasijevic A, Schiffner T, Zhang X, Lee WH, Torres JL, Zhang L, Irimia A, Copps J, Zhou KH, Kwon YD, Law WH, Schramm CA, Verardi R, Krebs SJ, Kwong PD, Doria-Rose NA, Wilson IA, Zwick MB, Yates JR, 3rd, Schief WR, Ward AB. 2020. HIV-1 envelope and MPER antibody structures in lipid assemblies. Cell Rep 31:107583.

73. Pan J, Peng H, Chen B, Harrison SC. 2020. Cryo-EM Structure of Full-length HIV-1 Env Bound With the Fab of Antibody PG16. J Mol Biol 432:1158-1168.

74. Long AR, O'Brien CC, Malhotra K, Schwall CT, Albert AD, Watts A, Alder NN. 2013. A detergent-free strategy for the reconstitution of active enzyme complexes from native biological membranes into nanoscale discs. BMC Biotechnol 13:41.

75. Knowles TJ, Finka R, Smith C, Lin YP, Dafforn T, Overduin M. 2009. Membrane proteins solubilized intact in lipid containing nanoparticles bounded by styrene maleic acid copolymer. J Am Chem Soc 131:7484-5.

76. Jamshad M, Grimard V, Idini I, Knowles TJ, Dowle MR, Schofield N, Sridhar P, Lin YP, Finka R, Wheatley M, Thomas OR, Palmer RE, Overduin M, Govaerts C, Ruysschaert JM, Edler KJ, Dafforn TR. 2015. Structural analysis of a nanoparticle containing a lipid bilayer used for detergent-free extraction of membrane proteins. Nano Res 8:774-789.

77. Lee SC, Knowles TJ, Postis VL, Jamshad M, Parslow RA, Lin YP, Goldman A, Sridhar P, Overduin M, Muench SP, Dafforn TR. 2016. A method for detergent-free isolation of membrane proteins in their local lipid environment. Nat Protoc 11:1149-62.

78. Orwick MC, Judge PJ, Procek J, Lindholm L, Graziadei A, Engel A, Grobner G, Watts A. 2012. Detergent-free formation and physicochemical characterization of nanosized lipid-polymer complexes: Lipodisq. Angew Chem Int Ed Engl 51:4653-7.

79. Postis V, Rawson S, Mitchell JK, Lee SC, Parslow RA, Dafforn TR, Baldwin SA, Muench SP. 2015. The use of SMALPs as a novel membrane protein scaffold for structure study by negative stain electron microscopy. Biochim Biophys Acta 1848:496-501.

80. Morrison KA, Akram A, Mathews A, Khan ZA, Patel JH, Zhou C, Hardy DJ, Moore-Kelly C, Patel R, Odiba V, Knowles TJ, Javed MU, Chmel NP, Dafforn TR, Rothnie AJ. 2016. Membrane protein extraction and purification using styrene-maleic acid (SMA) copolymer: effect of variations in polymer structure. Biochem J 473:4349-4360.

81. Jamshad M, Charlton J, Lin YP, Routledge SJ, Bawa Z, Knowles TJ, Overduin M, Dekker N, Dafforn TR, Bill RM, Poyner DR, Wheatley M. 2015. G-protein coupled receptor solubilization and purification for biophysical analysis and functional studies, in the total absence of detergent. Biosci Rep 35:e00188.

82. Qiu W, Fu Z, Xu GG, Grassucci RA, Zhang Y, Frank J, Hendrickson WA, Guo Y. 2018. Structure and activity of lipid bilayer within a membrane-protein transporter. Proc Natl Acad Sci U S A 115:12985-12990.

83. Nguyen HT, Qualizza A, Anang S, Zhao M, Zou S, Zhou R, Wang Q, Zhang S, Deshpande A, Ding H, Chiu TJ, Smith AB III, Kappes JC, Sodroski JG. 2022. Functional and highly cross-linkable HIV-1 envelope glycoproteins enriched in a pretriggered conformation. J Virol 96:e0166821.

84. Lin PF, Blair W, Wang T, Spicer T, Guo Q, Zhou N, Gong YF, Wang HG, Rose R, Yamanaka G, Robinson B, Li CB, Fridell R, Deminie C, Demers G, Yang Z, Zadjura L, Meanwell N, Colonno R. 2003. A small molecule HIV-1 inhibitor that targets the HIV-1 envelope and inhibits CD4 receptor binding. Proc Natl Acad Sci U S A 100:11013-8.

85. Lu M, Ma X, Reichard N, Terry DS, Arthos J, Smith AB III, Sodroski JG, Blanchard SC, Mothes W. 2020. Shedding-resistant HIV-1 envelope glycoproteins adopt downstream conformations that remain responsive to conformation-preferring ligands. J Virol 94:e00597-20.

86. Si Z, Madani N, Cox JM, Chruma JJ, Klein JC, Schon A, Phan N, Wang L, Biorn AC, Cocklin S, Chaiken I, Freire E, Smith AB III, Sodroski JG. 2004. Small-molecule inhibitors of HIV-1 entry block receptor-induced conformational changes in the viral envelope glycoproteins. Proc Natl Acad Sci U S A 101:5036-41.

87. Pancera M, Lai YT, Bylund T, Druz A, Narpala S, O'Dell S, Schon A, Bailer RT, Chuang GY, Geng H, Louder MK, Rawi R, Soumana DI, Finzi A, Herschhorn A, Madani N, Sodroski J, Freire E, Langley DR, Mascola JR, McDermott AB, Kwong PD. 2017. Crystal structures of trimeric HIV envelope with entry inhibitors BMS-

378806 and BMS-626529. Nat Chem Biol 13:1115-1122.

88. Nguyen HT, Wang Q, Anang S, Sodroski J. Characterization of the human immunodeficiency virus (HIV-1) envelope glycoprotein conformational states on infectious virus particles. J Virol, in the press.

89. Oluwole AO, Danielczak B, Meister A, Babalola JO, Vargas C, Keller S. 2017. Solubilization of membrane proteins into functional lipid-bilayer nanodiscs using a diisobutylene/maleic acid copolymer. Angew Chem Int Ed Engl 56:1919-1924.

90. Gulamhussein AA, Uddin R, Tighe BJ, Poyner DR, Rothnie AJ. 2020. A comparison of SMA (styrene maleic acid) and DIBMA (di-isobutylene maleic acid) for membrane protein purification. Biochim Biophys Acta Biomembr 1862:183281.

91. Walker LM, Phogat SK, Chan-Hui PY, Wagner D, Phung P, Goss JL, Wrin T, Simek MD, Fling S, Mitcham JL, Lehrman JK, Priddy FH, Olsen OA, Frey SM, Hammond PW, Protocol GPI, Kaminsky S, Zamb T, Moyle M, Koff WC, Poignard P, Burton DR. 2009. Broad and potent neutralizing antibodies from an African donor reveal a new HIV-1 vaccine target. Science 326:285-9.

92. Prabudiansyah I, Kusters I, Caforio A, Driessen AJ. 2015. Characterization of the annular lipid shell of the Sec translocon. Biochim Biophys Acta 1848:2050-6.

93. Nestorow SA, Dafforn TR, Frasca V. 2021. Biophysical characterisation of SMALPs. Biochem Soc Trans 49:2037-2050.

94. Dilworth MV, Findlay HE, Booth PJ. 2021. Detergent-free purification and reconstitution of functional human serotonin transporter (SERT) using diisobutylene maleic acid (DIBMA) copolymer. Biochim Biophys Acta Biomembr 1863:183602.

95. Gohain N, Tolbert WD, Orlandi C, Richard J, Ding S, Chen X, Bonsor DA, Sundberg EJ, Lu W, Ray K, Finzi A, Lewis GK, Pazgier M. 2016. Molecular basis for epitope recognition by non-neutralizing anti-gp41 antibody F240. Sci Rep 6:36685.

96. Leaman DP, Lee JH, Ward AB, Zwick MB. 2015. Immunogenic display of purified chemically cross-linked HIV-1 spikes. J Virol 89:6725-45.

97. Yuan W, Bazick J, Sodroski J. 2006. Characterization of the multiple conformational states of free monomeric and trimeric human immunodeficiency virus envelope glycoproteins after fixation by cross-linker. J Virol 80:6725-37.

98. Wang K, Zhang S, Go EP, Ding H, Wang WL, Nguyen HT, Kappes JC, Desaire H, Sodroski J, Mao Y. Asymmetric conformations of cleaved HIV-1 envelope

glycoprotein trimers in styrene-maleic acid lipid nanoparticles. Manuscript submitted.

99. Ma X, Lu M, Gorman J, Terry DS, Hong X, Zhou Z, Zhao H, Altman RB, Arthos J, Blanchard SC, Kwong PD, Munro JB, Mothes W. 2018. HIV-1 Env trimer opens through an asymmetric intermediate in which individual protomers adopt distinct conformations. Elife 7:e34271.

100. Madani N, Princiotto AM, Zhao C, Jahanbakhshsefidi F, Mertens M, Herschhorn A, Melillo B, Smith AB III, Sodroski J. 2017. Activation and inactivation of primary human immunodeficiency virus envelope glycoprotein trimers by CD4-mimetic compounds. J Virol 91:e01880-16.

101. Cale EM, Driscoll JI, Lee M, Gorman J, Zhou T, Lu M, Geng H, Lai YT, Chuang GY, Doria-Rose NA, Mothes W, Kwong PD, Mascola JR. 2022. Antigenic analysis of the HIV-1 envelope trimer implies small differences between structural states 1 and 2. J Biol Chem 298:101819.

1125 **Table 1. Antibodies recognizing HIV-1 Env epitopes.**

1126

Broadly neutralizing antibodies (bNAbs)

Antibody	Epitope
2G12	gp120 outer domain glycans
PGT121	gp120 V3 glycans
PG9 PG16 PGT145	gp120 V1/V2 quaternary (trimer apex)
VRC01 VRC03	gp120 CD4-binding site (CD4BS)
PGT151 35O22	gp120-gp41 interface
4E10 10E8	gp41 membrane-proximal external region (MPER)

Poorly neutralizing antibodies (pNAbs)

Antibody	Epitope
19b	gp120 V3
F105	gp120 CD4-binding site (CD4BS)
902090	gp120 V2 linear
17b	gp120 CD4-induced (CD4i)
F240	gp41 disulfide loop (Cluster I)

1127

1128

FIGURE LEGENDS

FIG 1 Antibody recognition of the 2-4 RM6 E Env on the cell surface. (A) A549 cells were induced with doxycycline to express 2-4 RM6 E Env. The cells were detached from the tissue-culture plates with 5 mM EDTA in 1x PBS. After pelleting and resuspension, the cells were aliquoted and incubated with the indicated antibodies. After washing, the cells were lysed in NP-40 lysis buffer and the cell lysates were incubated with Protein A-Sepharose beads. The precipitated antibody-Env complexes were Western blotted with a goat anti-gp120 antiserum (upper panel) or the human 4E10 anti-gp41 antibody (lower panel). The experiment was repeated twice and a typical result is shown. (B) The gp160 and gp120 bands in A were quantified using Fiji Image J (NIH). The intensities of the gp160 and gp120 bands precipitated by each antibody were normalized to those of the respective gp160 and gp120 bands precipitated by the PGT121 antibody. The means and standard deviations of the results of two independent experiments are shown.

FIG 2 Antigenicity profiles of HIV-1 Envs on purified cell membranes. (A) A549 cells were induced with doxycycline to express the wt HIV-1_{AD8} Env or the 2-4 RM6 E Env. Cell membranes were purified as described in Materials and Methods and incubated with the indicated antibodies for 1 h at 4°C, with or without 10 μM BMS-806. The membranes were lysed with 1% NP-40 with or without BMS-806 for 5 minutes on ice, and then incubated with Protein A-Sepharose beads for 1 h at 4°C. The precipitated proteins were subjected to Western blotting with a goat anti-gp120 antiserum or the human 4E10 anti-gp41 antibody. (B) The intensities of the gp120 and gp160 bands in A were measured in Fiji Image J (NIH). The gp120 and gp160 band intensity for each

antibody was normalized to those of the respective gp120 and gp160 bands of the PGT121 samples. The means and standard deviations from two independent experiments are shown.

FIG 3 Properties of amphipathic copolymers for membrane protein solubilization. The structures and properties of the SMA and DIBMA variants used in this study are shown.

FIG 4 Yield and antigenicity of the AE.2 Env solubilized in different amphipathic copolymers. A549 cells were induced with doxycycline to express the AE.2 Env. Cell membranes were purified, crosslinked with 0.35 mM DTSSP and extracted with the indicated amphipathic copolymers. (A) Eluates from the Ni-NTA beads were analyzed by SDS-PAGE under non-reducing (-DTT) or reducing (+DTT) conditions, followed by silver staining. (B) A small panel of antibodies was used to assess the antigenicity of the AE.2 Env eluted from the Ni-NTA beads. The 2G12 bNAb recognizes gp120 outer domain glycans in a manner that is relatively independent of Env conformation. The 19b pNAb recognizes a gp120 V3 epitope. The PGT145, PG9 and VRC03 bNAbs exhibit some preference for the pretriggered (State-1) Env conformation. The AE.2 Env precipitated by the antibodies was captured on Protein A-Sepharose beads and subjected to Western blotting with a goat anti-gp120 antiserum. The results of a typical experiment are shown.

FIG 5 Stability of Env solubilized in Cymal-5, SMA or RIPA at different temperatures. To evaluate the integrity of the cleaved Env trimer under different

solubilization conditions, we compared the relative efficiencies of gp120 and gp160 precipitation by Ni-NTA beads, which bind the His_6 tags at the carboxyl termini of the Envs. (A) A549 cells were induced with doxycycline to express the wt HIV-1_{AD8} and 2-4 RM6 E Envs, both of which have His_6 tags at the carboxyl terminus. Forty-eight hours after induction, the cells were lysed in 1% Cymal-5, 1% SMA or RIPA buffer in the absence or presence of 10 μM BMS-806 for 5 minutes on ice. After pelleting cell debris, a sample of the supernatant was saved as "Input." The remainder of the cleared supernatants was incubated at the indicated times and temperatures with Ni-NTA beads by end-over-end rotation. For Cymal-5, SMA and RIPA samples, the beads were washed with 60 bed volumes of the corresponding wash buffers (20 mM Tris-HCl (pH 8.0), 100 mM $(NH_4)_2SO_4$, 1 M NaCl, 30 mM imidazole, 1% Cymal-5); (20 mM Tris-HCl (pH 8.0), 100 mM $(NH_4)_2SO_4$, 1 M NaCl, 30 mM imidazole, 0.005% Cymal-6); or RIPA buffer. After washing, the samples captured on the Ni-NTA beads were Western blotted with a goat anti-gp120 antiserum (upper panels) or the human 4E10 anti-gp41 antibody (lower panels). RT – room temperature. (B) Quantification of the gp120 and gp160 band intensity in A was performed in Fiji Image J (NIH). The stability of the Env trimer was calculated by the formula $(gp120/gp160)_{Ni\text{-}NTA} \div (gp120/gp160)_{Input}$. The means and standard deviations derived from two independent experiments are shown. The data were compared with a Student's t test. Two-tailed P values are shown, *: $P<0.05$; **: $P<0.01$; ***: $P<0.001$.

FIG 6 Oligomeric composition of the 2-4 RM6 E Env in Cymal-5 and SMA at room temperature. Membranes were prepared from A549 cells induced with doxycycline to express the 2-4 RM6 E Env. The 2-4 RM6 E Env was extracted at room temperature with 1% SMA or 1% Cymal-5. The extracted Envs were purified on Ni-NTA beads at room temperature and analyzed by SDS-PAGE (A) or Blue Native-PAGE (B), followed by silver staining. Note that BMS-806 treatment shifts the Env trimer population to a form that migrates faster on Blue Native gels.

FIG 7 Antigenicity of the 2-4 RM6 E Env after Ni-NTA purification from cell lysates. (A) A549 cells were induced with doxycycline to express the 2-4 RM6 E Env. Forty-eight hours later, the cells were lysed with either 1% Cymal-5 or 1% SMA in the absence or presence of 10 μM BMS-806. The 2-4 RM6 E Env was partially purified by Ni-NTA affinity chromatography, aliquoted and incubated with the indicated antibodies together with Protein A-Sepharose beads for 1 h at 4°C. An aliquot without added antibody served as the Input sample. The Input sample and precipitated proteins were Western blotted with a goat anti-gp20 antiserum (upper panels) and the human 4E10 anti-gp41 antibody (lower panels). The asterisk marks the position of the heavy chains of the antibodies used for precipitation. (B) Quantification of the intensity of the gp120 and gp160 bands in A was performed in Fiji Image J (NIH). The intensities of the gp120 and gp160 bands were normalized to those of the respective gp120 and gp160 bands precipitated by the PGT121 antibody. The means and standard deviations derived from two independent experiments are shown.

FIG 8 Comparison of the 2-4 RM6 E Env conformation in Cymal-5 and SMA. The correlation is shown between the antigenicities of the Cymal-5-solubilized and SMA-solubilized cleaved 2-4 RM6 E Envs in the absence (A,B) or presence (C) of 10 μM BMS-806. The pNAbs are designated in red and the bNAbs in blue. The Spearman rank correlation coefficient (r_S), the Pearson r (r_P) and two-tailed P values are shown. In A, note the outlier values for the two bNAbs (4E10 and 10E8) directed against the gp41 MPER (highlighted by the box). In B, the correlation is shown for the antibodies other than the MPER-directed 4E10 and 10E8 anti-gp41 antibodies.

FIG 9 Effect of crosslinking on the antigenicity of 2-4 RM6 E Env-SMALPs prepared from purified membranes. (A) A549 cells were induced with doxycycline to express the 2-4 RM6 E Env. Cell membranes were purified and divided into two parts, one treated with 0.35 mM DTSSP crosslinker at room temperature for 45 minutes and the other mock-treated. DTSSP crosslinks are able to be reduced, allowing crosslinked gp120 and gp41 subunits to be distinguished from uncleaved gp160 on Western blots. The membranes were lysed in 1% SMA in the presence of 10 μM BMS-806 for 30 minutes at room temperature. The 2-4 RM6 E Env was purified by Ni-NTA affinity chromatography, aliquoted and incubated with the indicated antibodies together with Protein A-Sepharose beads for 1 h at 4°C. The precipitated proteins were analyzed on reducing SDS-polyacrylamide gels and Western blotted with a goat anti-gp120 antiserum (upper panels) and the human 4E10 anti-gp41 antibody (lower panels). The asterisk indicates the position of the heavy chain of the precipitating antibodies. (B) Quantification of gp120 and gp160 band intensity in A was performed in Fiji Image J

(NIH). The intensities of the gp120 and gp160 bands were normalized to those of the respective bands precipitated by the PGT121 antibody. The means and standard deviations derived from two independent experiments are shown.

FIG 10 Antigenicity of Env purified using multiple measures to preserve Env conformation. (A) Cell membranes were purified from A549 cells induced with doxycycline to express the 2-4 RM6 E Env. The purified membranes were crosslinked with 0.35 mM DTSSP in the presence of 10 μM BMS-806 at room temperature for 45 minutes. The membranes were lysed in 1% SMA in the presence of 10 μM BMS-806 for 30 minutes at room temperature. The 2-4 RM6 E Env was purified from the membrane lysates by Ni-NTA affinity chromatography. In A, a fraction of the purified Env was saved as Input and the rest was used to evaluate the binding of the indicated antibodies, as described in the Figure 8 legend. In B, the purified Env was incubated with 40 μg/ml each of the 19b and F240 pNAbs together with Protein A-Sepharose beads for 30 minutes at room temperature. After 19b/F240 counterselection, the flow-through sample was aliquoted, with one fraction serving as the Input sample and the rest used to evaluate antigenicity, as described in the Figure 8 legend. The bar graph shows the relative binding to gp120 and gp160 normalized to the respective bands for the PGT121 antibody. The means and standard deviations from two experiments are reported.

FIG 11 A model for the effect of extraction from membranes on HIV-1 Env conformation. The cleaved membrane Env of primary HIV-1 mainly occupies a pretriggered (State-1) conformation. Upon solubilization of the membrane proteins by

SMA or Cymal-5 at 4°C, the extracted Envs assume conformations (States X_S and X_C, respectively) that differ from State 1. The conformations of the Envs in SMALPs and Cymal-5 resemble one another, with differences mainly confined to the membrane-proximal Env elements. The resemblance of the Envs solubilized by distinct approaches supports the existence of a default Env conformation that is assumed when State 1 is destabilized by the loss of the membrane. BMS-806 can bring the solubilized Envs closer to a State-1 conformation, but BMS-806-treated, solubilized Envs still differ from State 1. When the temperature is raised to room temperature, Envs in SMALPs are more stable than Envs in detergents like Cymal-5.

Figure 1

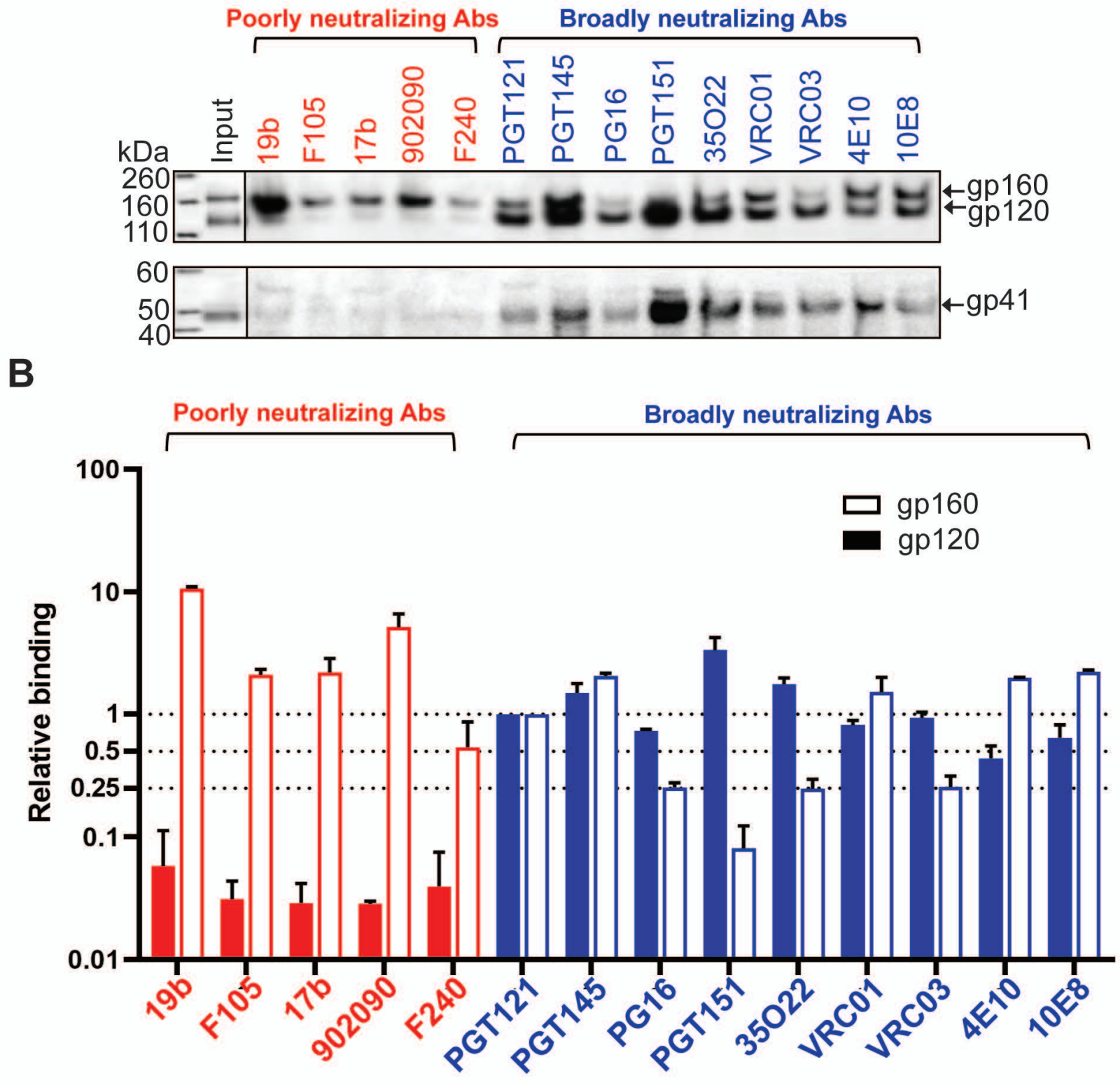
A Cell-surface 2-4 RM6 E Env
Poorly neutralizing Abs
Broadly neutralizing Abs
Input
19b
F105
17b
902090
F240
PGT121
PGT145
PG16
PGT151
35O22
VRC01
VRC03
4E10
10E8
kDa
260
160
110
60
50
40
gp160
gp120
gp41
B
Poorly neutralizing Abs
Broadly neutralizing Abs
gp160
gp120
Relative binding
100
10
1
0.5
0.25
0.1
0.01
19b
F105
17b
902090
F240
PGT121
PGT145
PG16
PGT151
35O22
VRC01
VRC03
4E10
10E8

Figure 2

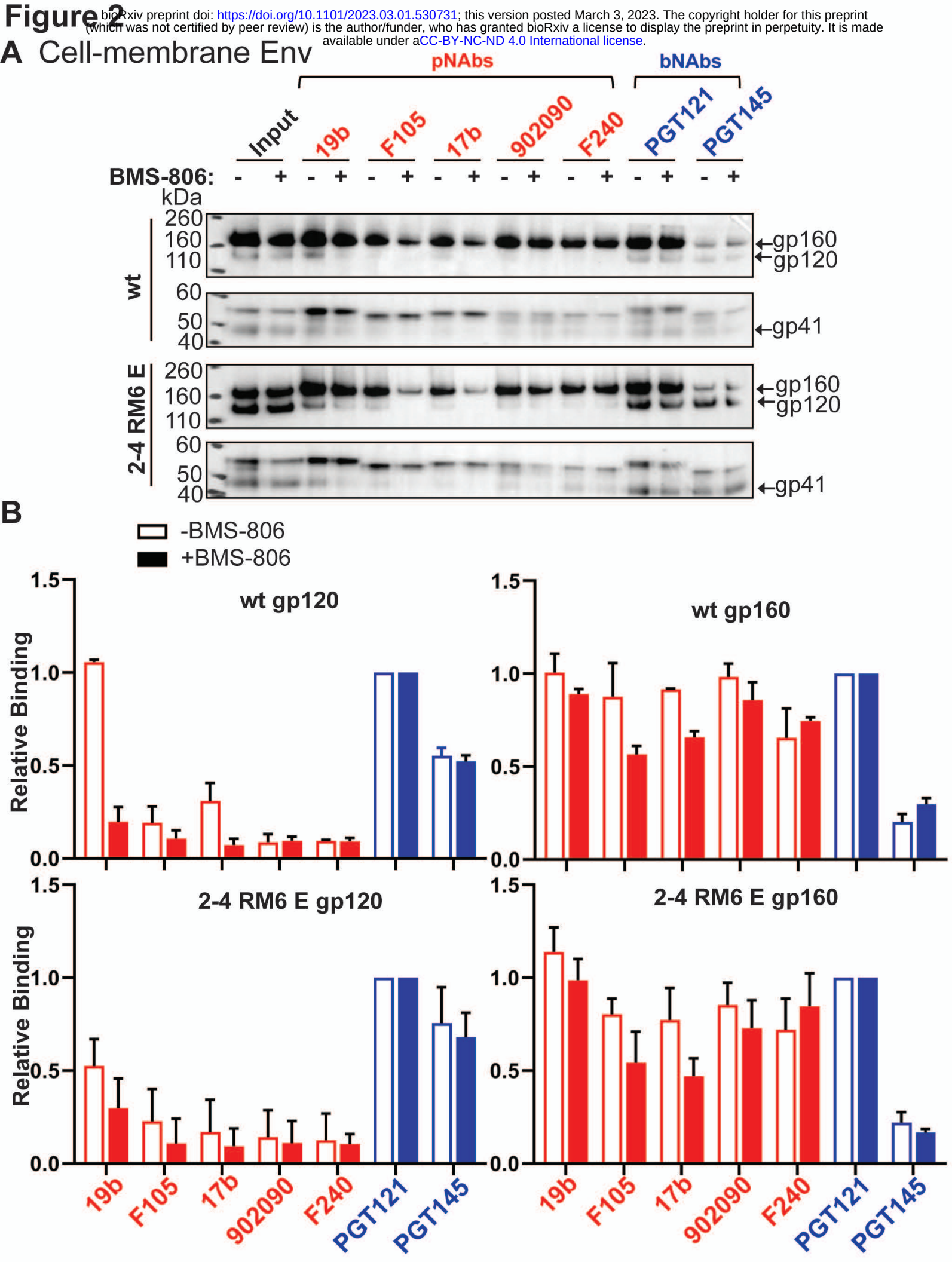

Figure 3

	Styrene: Maleic Acid ratio	Molecular Weight (kDa)	pH	Divalent Ion Tolerance
DIBMA 10		10	7.5	<25 mM
DIBMA 12		12		<25 mM
DIBMA Glycerol		10		>50 mM
DIBMA Glucosamine		10		>50 mM
SMALP 1100I	1.4:1	5		<100 mM
SMALP 25010	3:1	10		<5 mM
SMALP 30010	2.3:1	6.5		<5 mM
SMALP 40005	1.4:1	5		<5 mM
In-house SMA	2:1			

DIBMA 10 or DIBMA 12

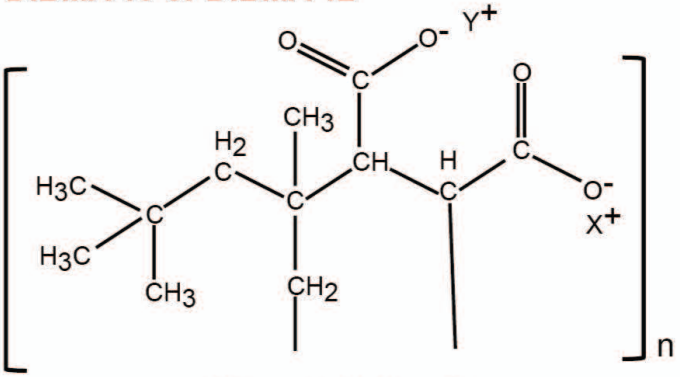

X=Na or H Y=Na or H

DIBMA Glycerol

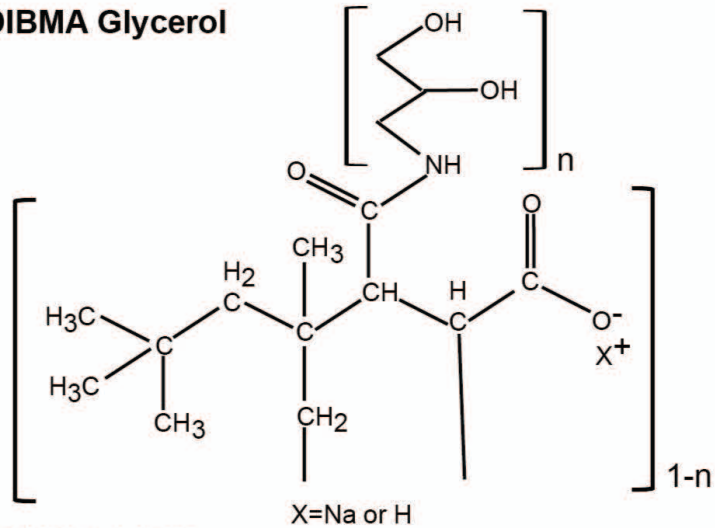

X=Na or H

DIBMA Glucosamine

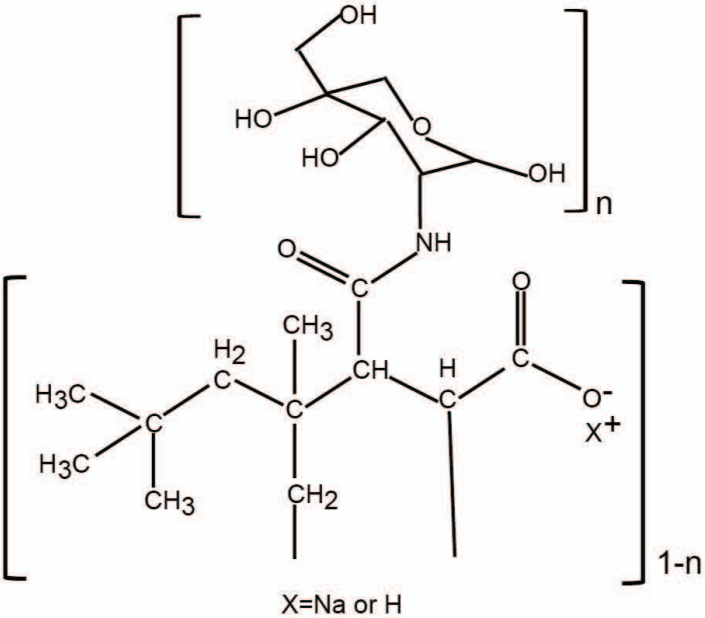

X=Na or H

SMALP 1100I

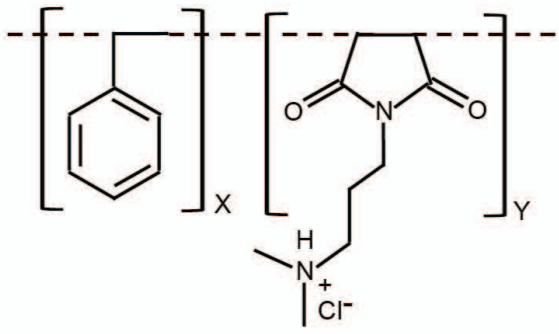

SMALP 25010/30010/40005 or In-house SMA

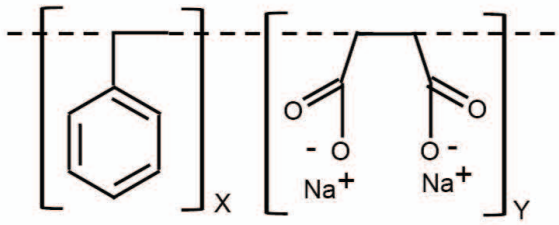

Figure 4

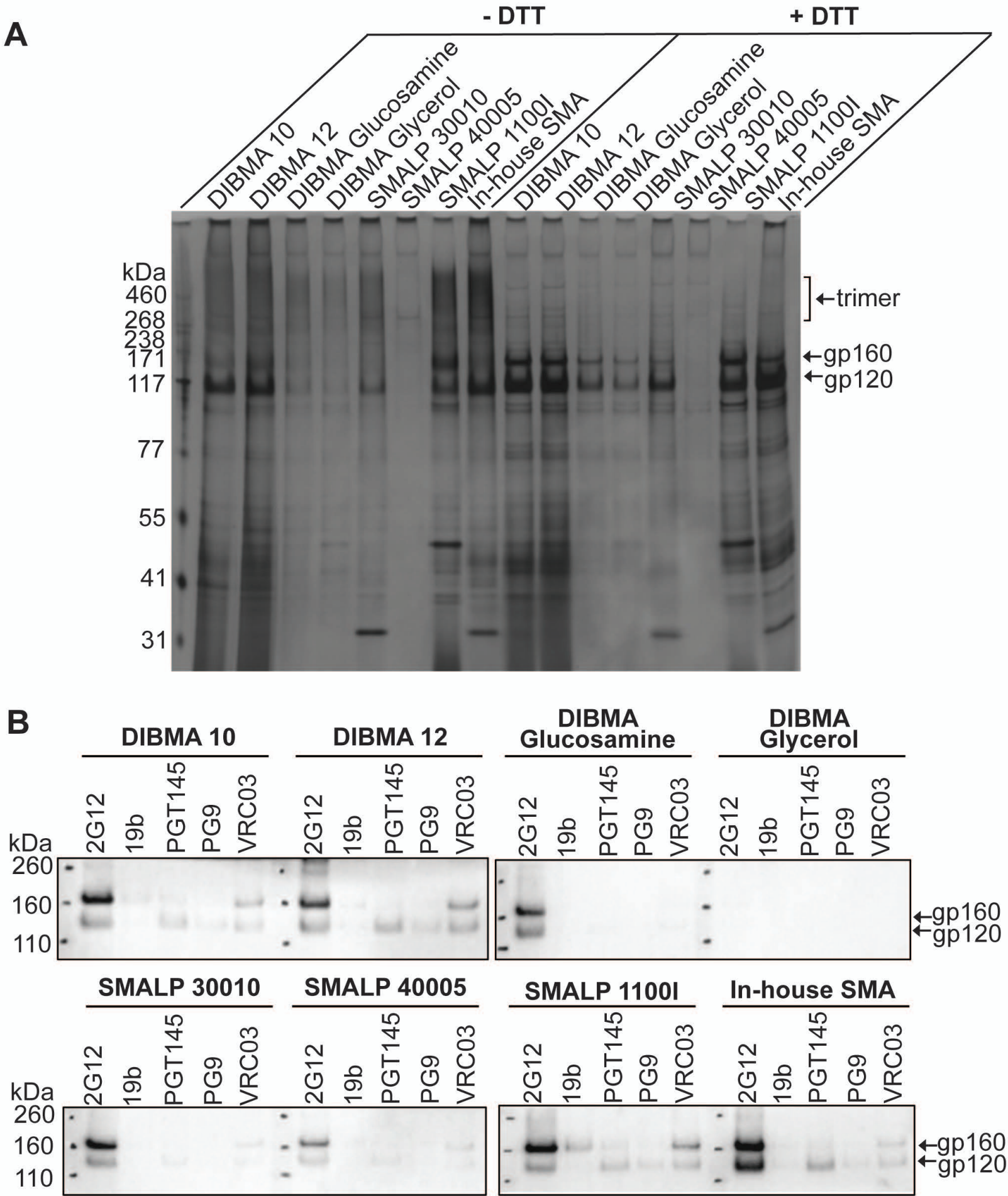
A
- DTT
+ DTT
DIBMA 10
DIBMA 12
DIBMA Glucosamine
DIBMA Glycerol
SMALP 30010
SMALP 40005
SMALP 1100I
In-house SMA
kDa
460
268
238
171
117
77
55
41
31
trimer
gp160
gp120
B
DIBMA 10
DIBMA 12
DIBMA Glucosamine
DIBMA Glycerol
SMALP 30010
SMALP 40005
SMALP 1100I
In-house SMA
2G12
19b
PGT145
PG9
VRC03
kDa
260
160
110
gp160
gp120

Figure 5

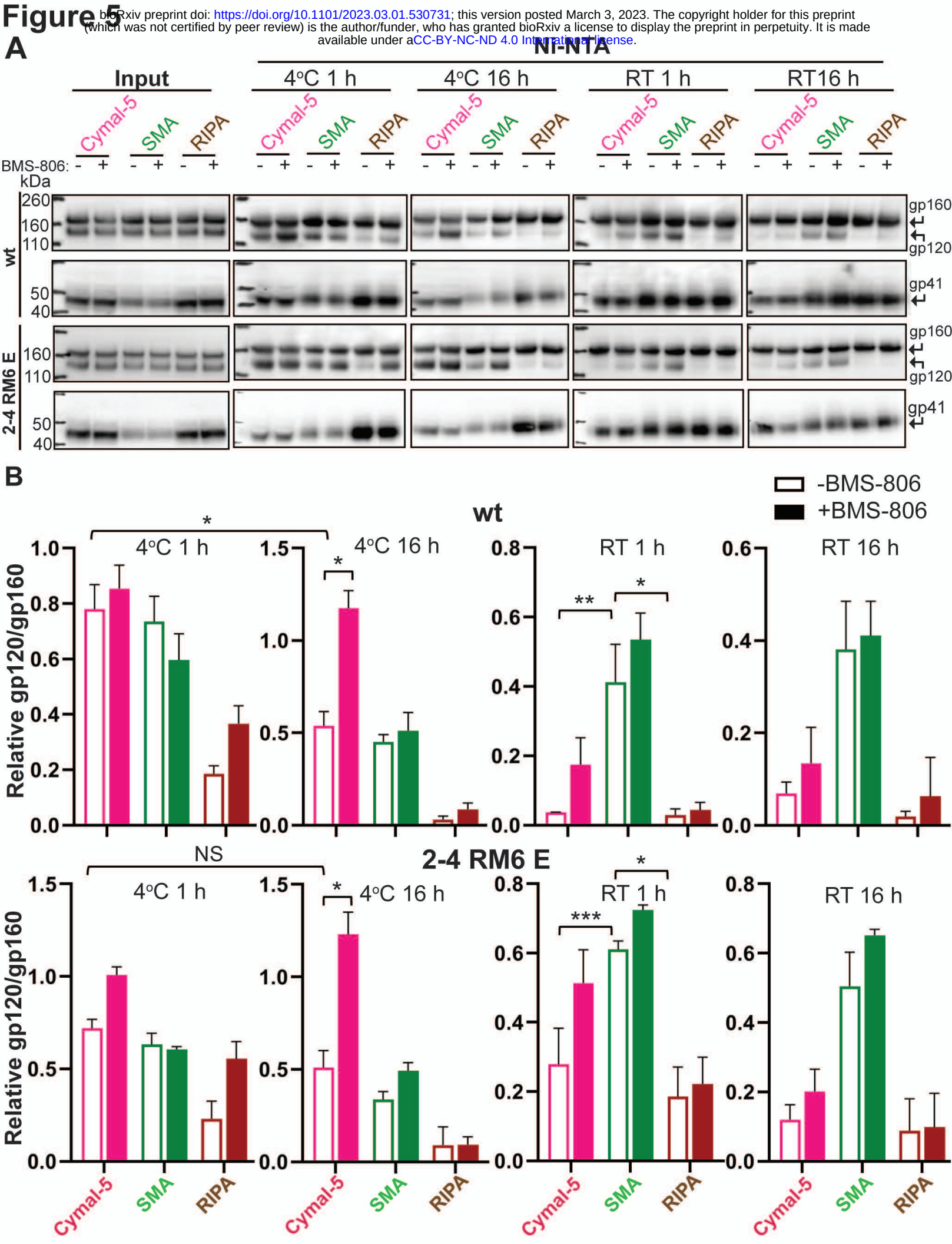

Figure 6

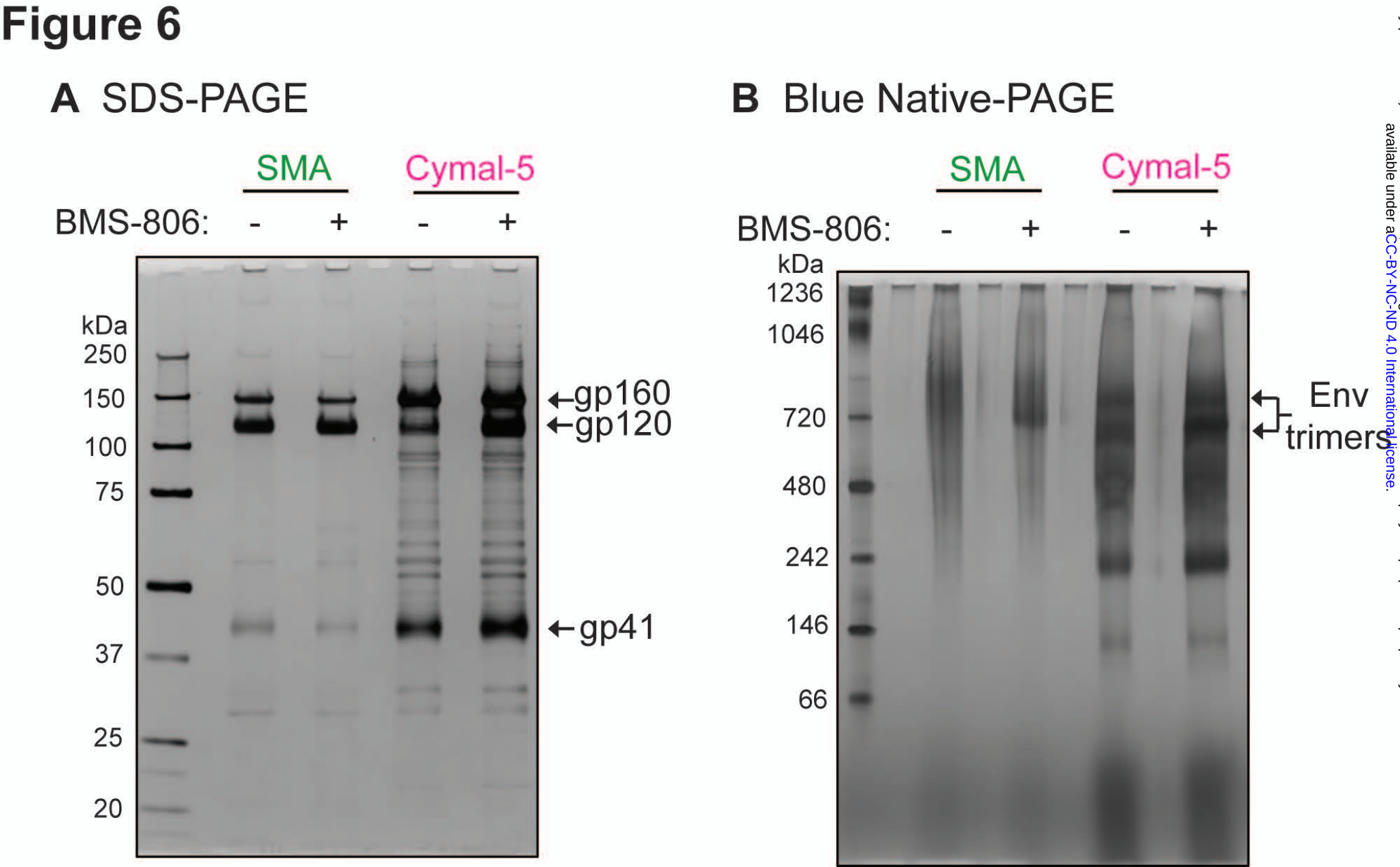

Figure 7

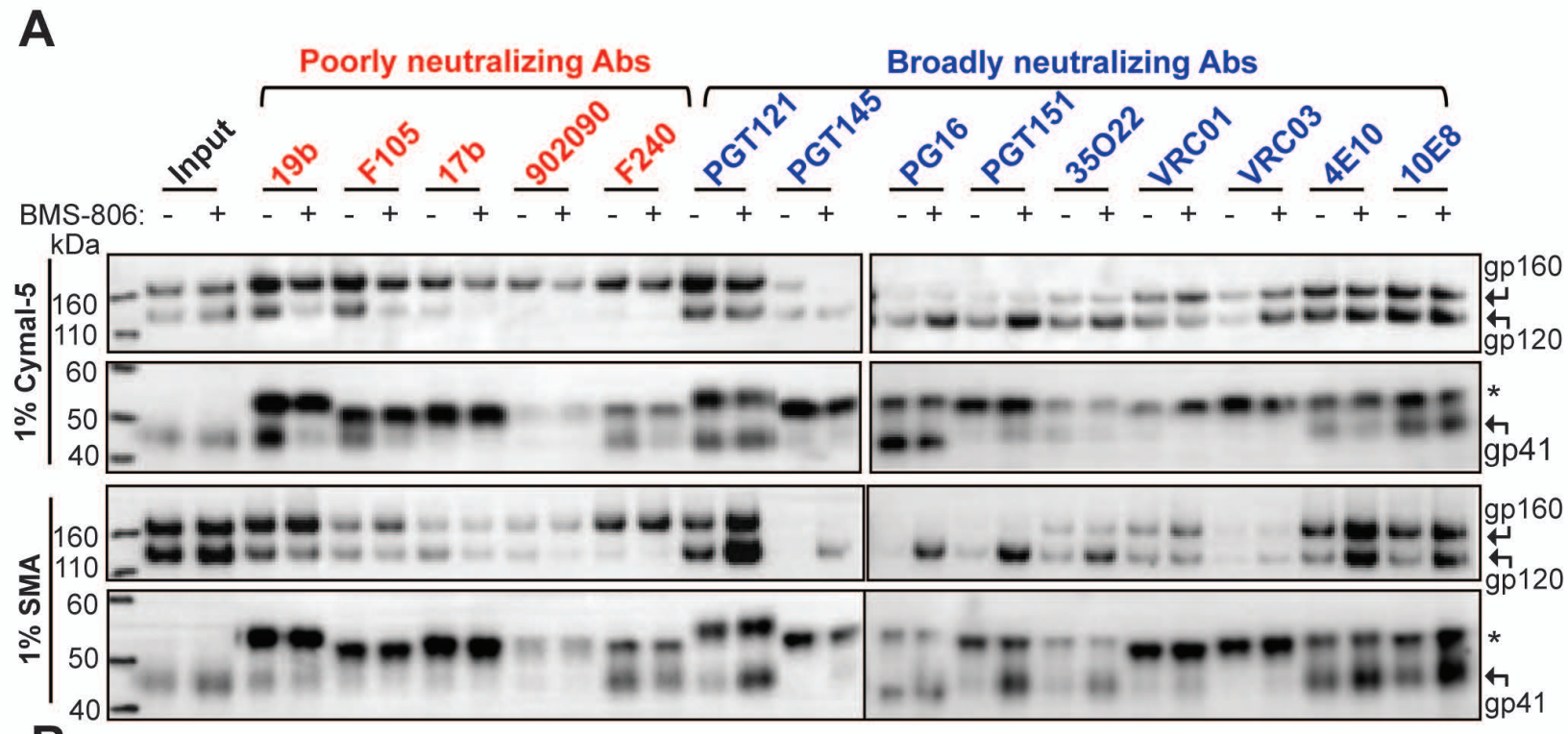

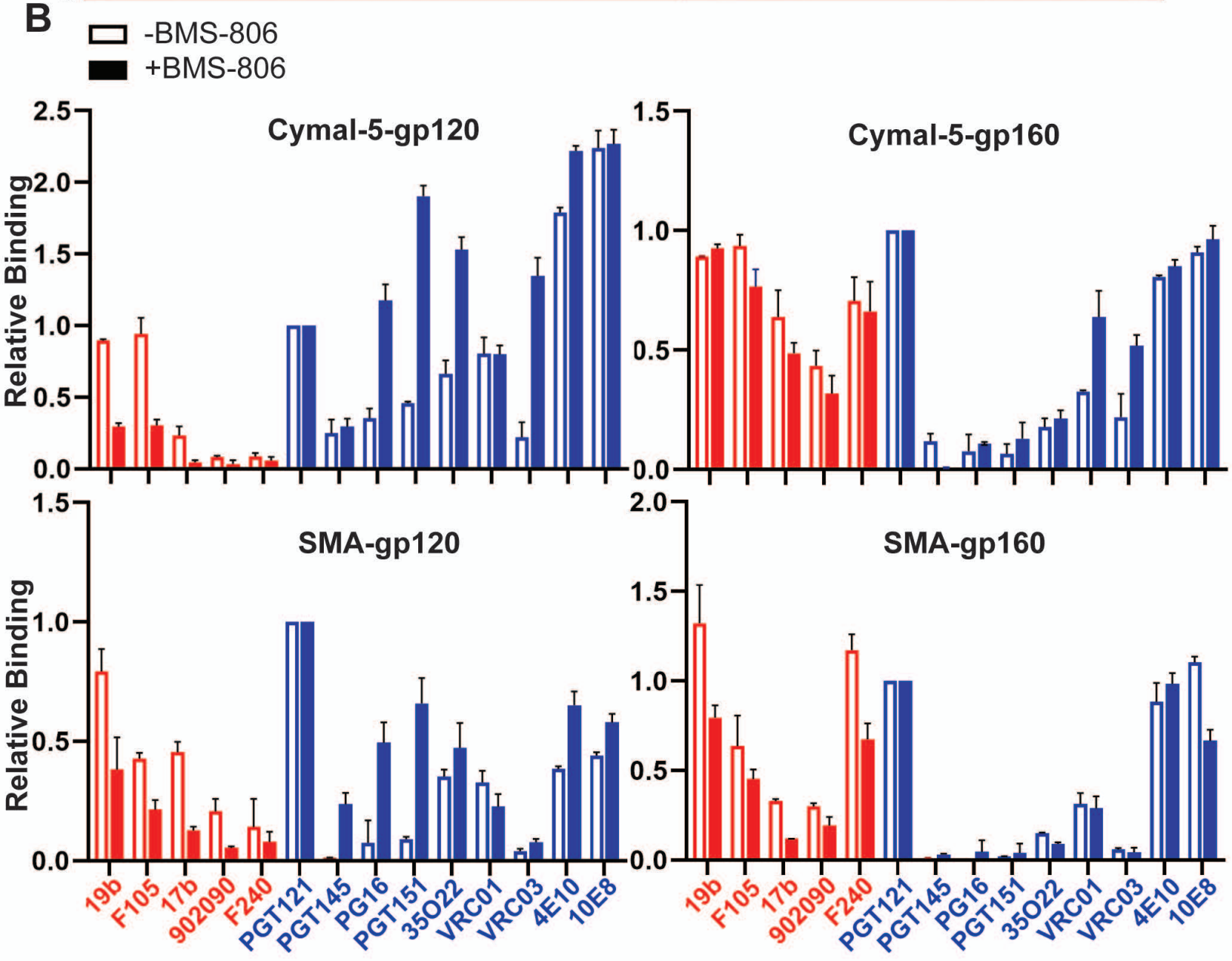

Figure 8

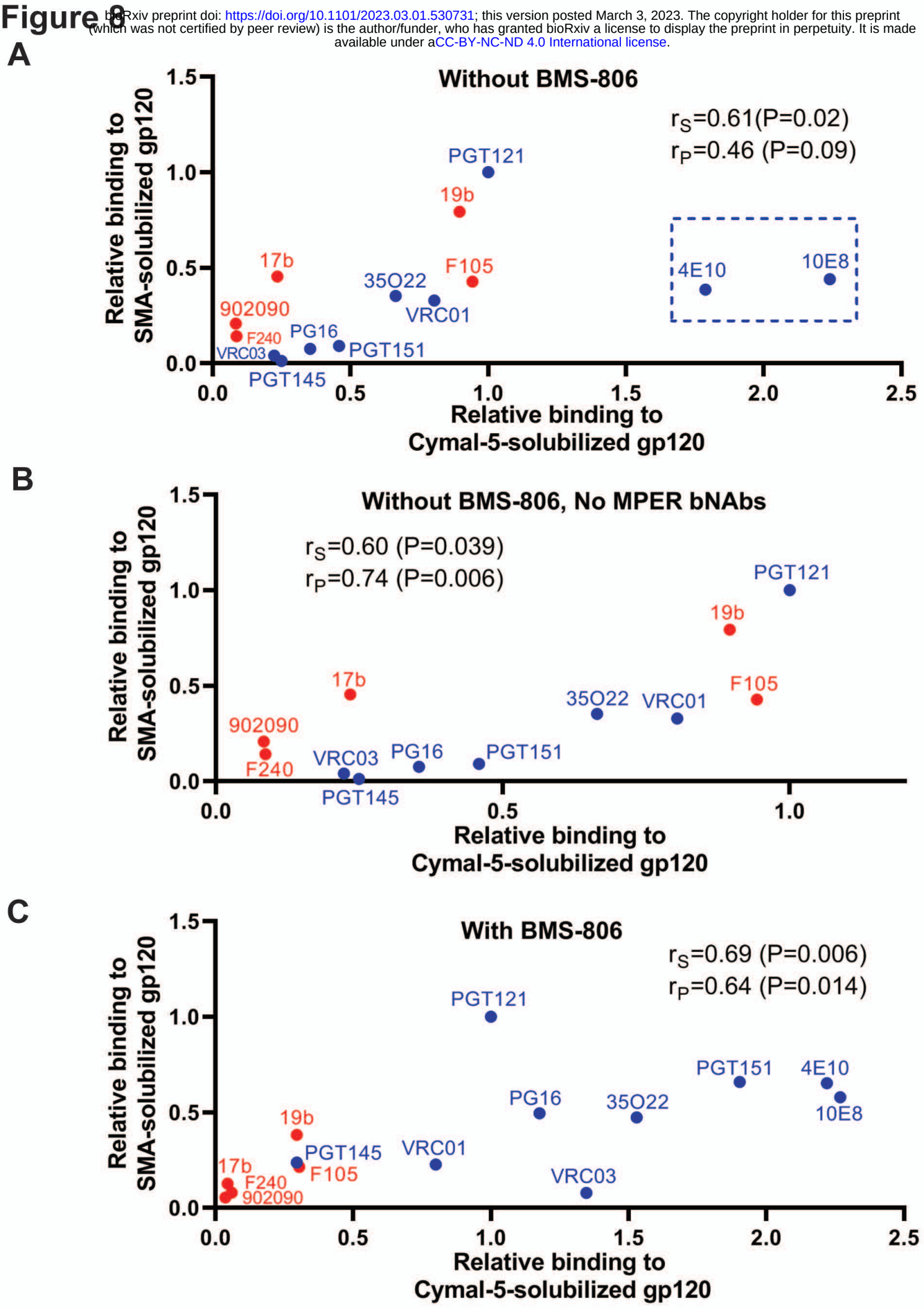

Figure 9

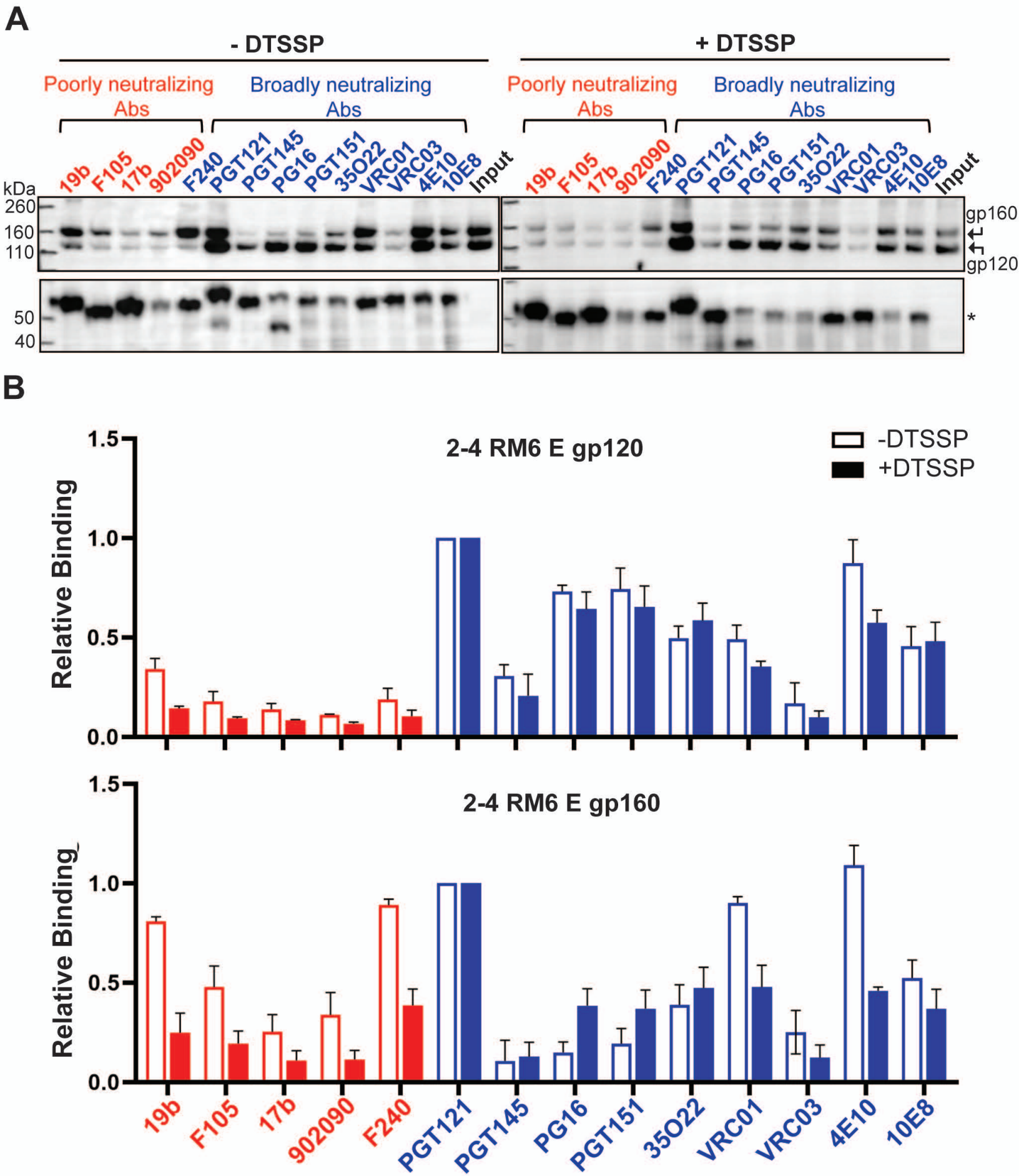

Figure 10

A No counterselection

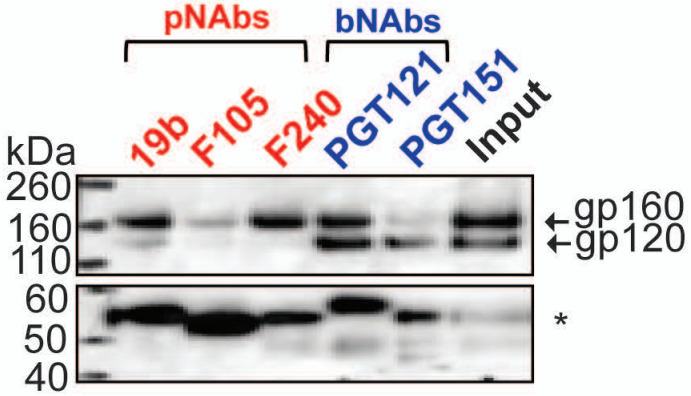

B With 19b/F240 counterselection

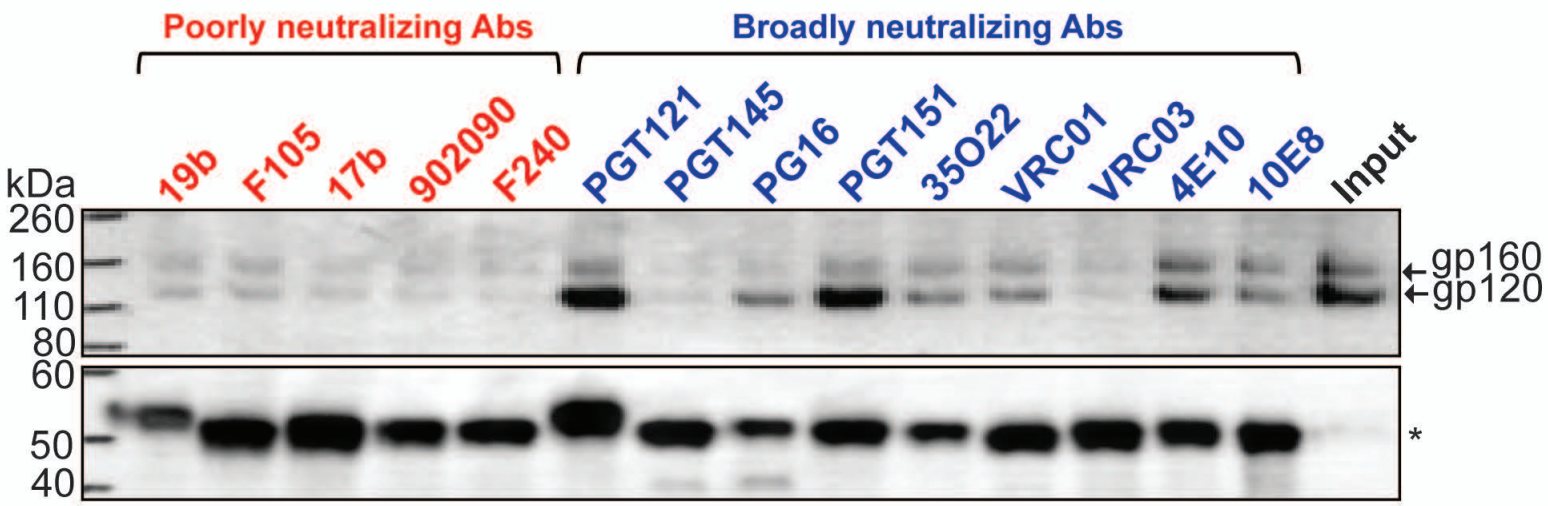

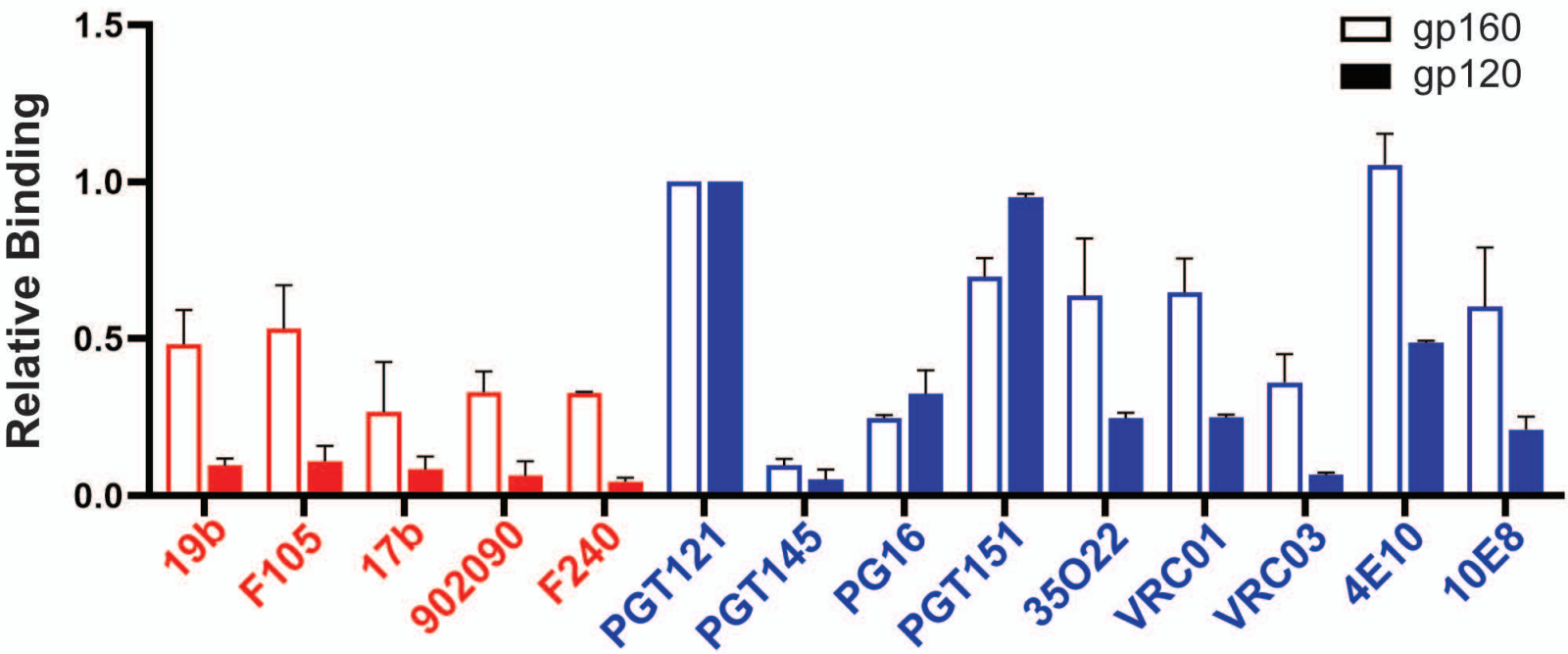

Figure 11

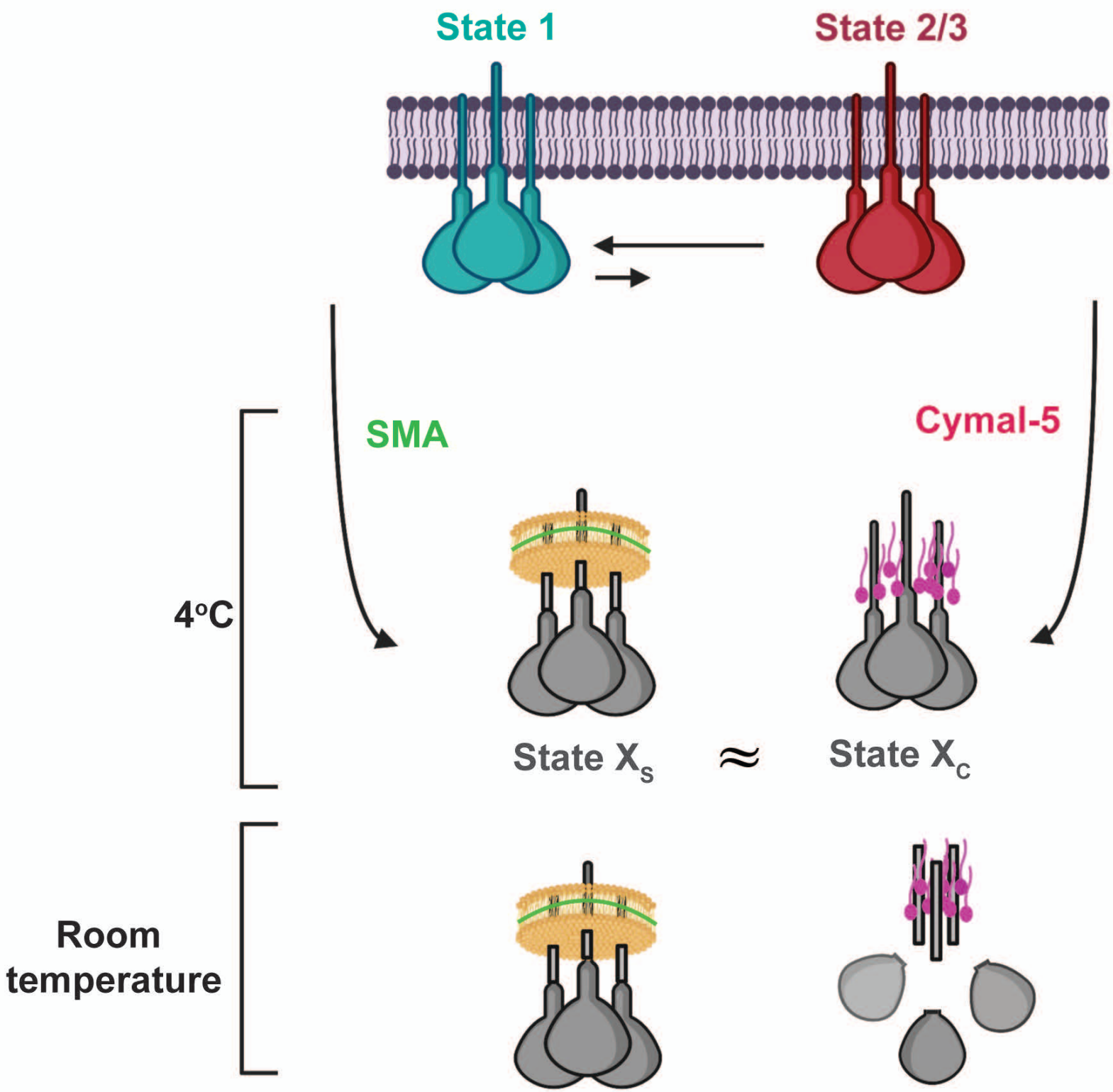
State 1
State 2/3
SMA
Cymal-5
4°C
State X_s
≈
State X_c
Room temperature